Time-Shared NMR Experiments

TEODOR PARELLA, PAU NOLIS

Servei de Ressonància Magnètica Nuclear, Universitat Autònoma de Barcelona, Bellaterra E-08193, Barcelona, Spain

ABSTRACT: Details on the implementation of the simultaneous evolution of multiple frequencies into the same time period of a NMR pulse sequence are introduced. Time-shared (TS) versions of the most useful inverse 2D NMR experiments (TS-HMBC, TS-HSQC, TS-HSQC-TOCSY, and TS-HSQMBC) are presented and illustrated for simultaneous acquisition of $^{1}H/^{13}C$ and $^{1}H/^{15}N$ NMR spectra. The major benefits associated to the parallel acquisition of multiple spectra from a single NMR experiment are spectrometer time savings and the achievement of multiple and complementary information with improved sensitivity gains per time unit. © 2010 Wiley Periodicals, Inc. Concepts Magn Reson Part A 36A: 1–23, 2010.

KEY WORDS: time-sharing; HSQC; HMBC; HSQC-TOCSY; HSQMBC; IPAP; coupling constants

INTRODUCTION

It is widely known that the Achilles' heel of NMR spectroscopy is the low sensitivity when compared with other analytical techniques. Nevertheless, much effort has been done from earlier days to superimpose to that problem. Nowadays, NMR enjoys from all improvements done along the history at different research fields, mainly focused on methodological and technical advances. In this sense, the versatile design of new and improved pulse sequences offering better sensitivity/resolution or providing new information has been one of the most changeable fields. Now, the pool of high-resolution NMR experiments to be used for structure elucidation of both small, natural-abundance chemical molecules (*1*) and large, isotopically labeled biomolecules (*2*) is well established. On the other hand, the development of improved data acquisition NMR protocols is an important area of current research to obtain maximum information in more reduced spectrometer times. Some requirements for the successful use of these new methods should be a general applicability, robust implementation on a variety of conditions, and full automation for routine use. Signal enhancement in NMR has been traditionally achieved by signal averaging followed by Fourier transformation of the time-domain data, combined with homonuclear and heteronuclear polarization transfer or NOE methods. Probably, the last important revolution in NMR pulse sequence design was the incorporation of pulsed field gradients as powerful elements for a better efficient coherence selection and purging in many homo- and heteronuclear multidimensional experiments (*1*, *2*).

Recently, some old concepts successfully implemented in other areas of the NMR have

Received 21 May 2009; revised 29 September 2009; accepted 1 October 2009

Correspondence to: Teodor Parella. E-mail: teodor.parella@uab.cat

Concepts in Magnetic Resonance Part A, Vol. 36A(1) 1–23 (2010)

Published online in Wiley InterScience (www.interscience.wiley.com). DOI 10.1002/cmr.a.20150

© 2010 Wiley Periodicals, Inc.

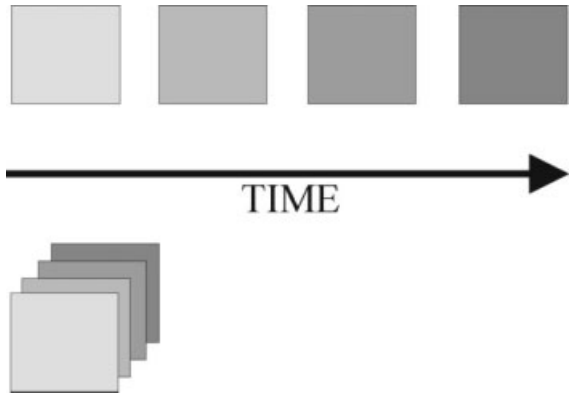

Figure 1 Sequential vs. parallel NMR data acquisition. Simultaneous recording of multiple spectra can afford spectrometer time savings and facilitate automation.

been adapted to accelerate even more data acquisition in high-resolution NMR spectroscopy (*3*). Some examples should be the rapid pulsing combined with Ernst angle excitation (*4*), simultaneous acquisition of related experiments using Hadamard encoding (*5*), fast acquisition of multidimensional experiments using the reduced dimensionality (RD) approach combined with GFT (*6*), spectral reconstruction methods using projection-reconstruction (*7*) or nonlinear data sampling (*8*) techniques or collection of different experiments in different parts of the same sample using spatial encoding (known as single-scan NMR) (*9*), among others. In addition, it has also been demonstrated that the combination of some of these techniques can afford accumulative advantages (*10*, *11*).

The classical strategy for NMR data acquisition is the sequential acquisition of individual experiments. Simultaneous or parallel acquisition of different but related NMR experiments could afford multiple and complementary information in a single-shot acquisition (Fig. 1). For instance, it can be advisable to record $^{1}H/^{13}C$ and $^{1}H/^{15}N$ HMBC spectra in many nitrogen-containing compounds, such as natural products, peptides and proteins, synthetic organic derivatives, organometallic and inorganic molecules, nucleotides, or nucleic acids. Both pulse sequences present strong similarities, and the possibility to simultaneously acquire both spectra by redesigning the original HMBC pulse

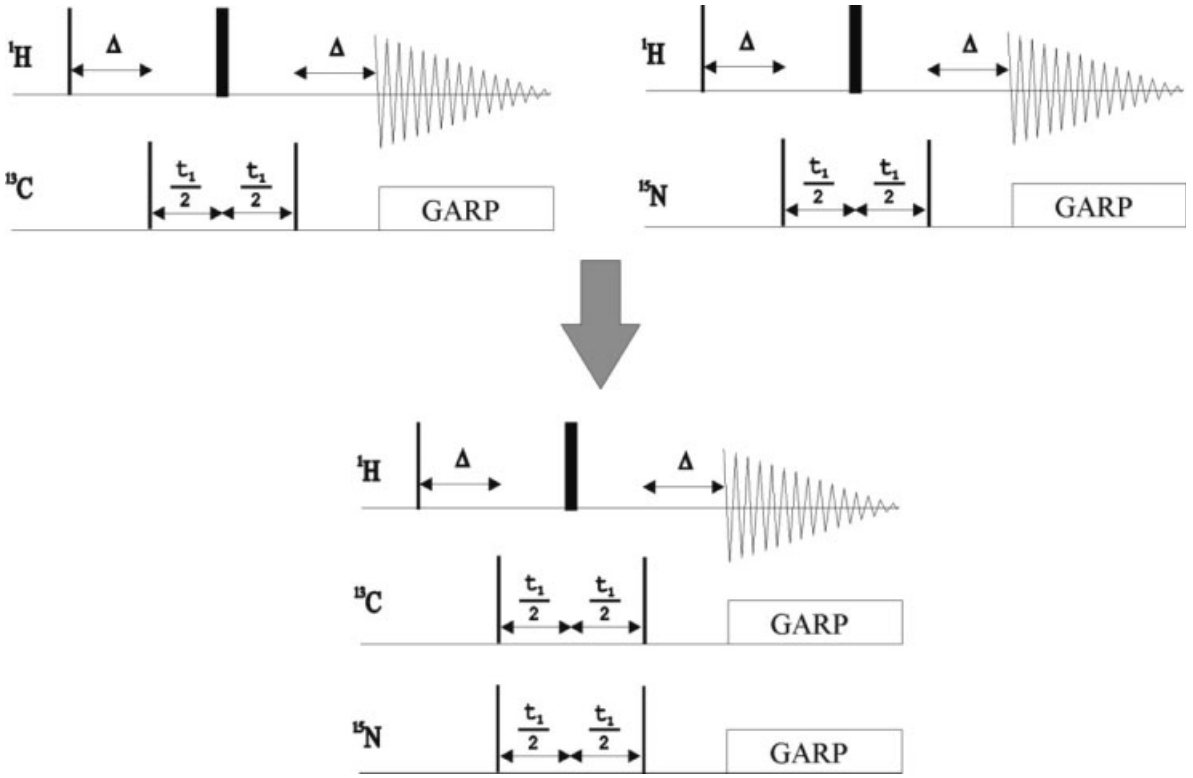

Figure 2 Conversion of two independent but complementary HMQC pulse sequences in a single one by using the concept of time-sharing (TS) multiple-frequency evolution during a variable t_1 evolution period. The number of additional pulses or delays should be keep at a minimum to obtain reliable sensitivity gains per time unit.

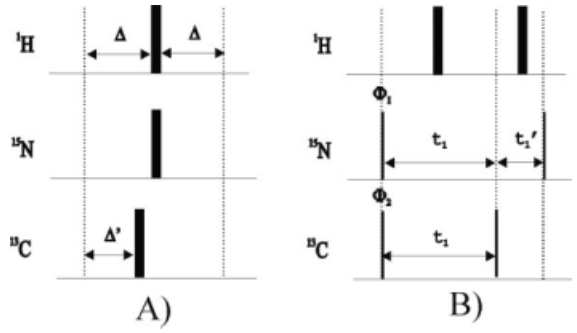

Figure 3 Basic building blocks to be implemented in time-shared NMR experiments. (A) Concatenated ^{13}C,^{15}N INEPT-like element. This is a fixed-optimized time period for the simultaneous evolution of different sized J(NH) and J(CH) coupling constants. (B) Incremented time period to allow simultaneous evolution of ^{13}C and ^{15}N chemical shift as a function of their spectral widths: $\Delta t_1 = 1/\mathrm{SW}(^{13}\mathrm{C})$ and $\Delta t_1' = 1/\mathrm{SW}(^{15}\mathrm{N}) - 1/\mathrm{SW}(^{13}\mathrm{C})$. Differentiation between C and N cross peaks is performed by nucleus editing (proper choice of the ϕ_1 and ϕ_2 phases as illustrated in Fig. 5).

sequence timings would considerably reduce the total acquisition time.

Several years ago, a different number of works described the fundamentals of time-shared (TS) multiple-frequency evolution in proton-detected experiments (*12–20*). Herein, the basic concepts of TS evolution will be described and examples will be provided for the simultaneous acquisition of modern ^{1}H/^{13}C and ^{1}H/^{15}N NMR spectra in small-molecule NMR. We also provide details on the implementation of the TS concept into the most conventional proton-detected inverse NMR experiments such as, for instance, TS-HSQC, TS-HSQC-TOCSY, TS-HMBC, and TS-HSQMBC experiments. Simple modifications of these basic schemes allow the incorporation of IPAP editing simultaneously for ^{13}C and ^{15}N as a useful tool for the simultaneous measurement of direct or long-range CH and NH coupling constants. Finally, the combination of the TS principles with other accelerated acquisition methods can provide new approaches for acquisition of multiple and complementary NMR data in reduced acquisition times.

RESULTS AND DISCUSSION

The Concept of Time-Sharing Evolution

The basic four-pulse HMQC pulse sequence will be used to introduce the concept of TS. Figure 2 shows the basic conversion between two separate ^{13}C and ^{15}N HMQC pulse trains to a single TS version. The resulting TS-HMQC experiment would result to overlap the ^{13}C and the ^{15}N pulse sequence. Although the sequential acquisition of two equivalent NMR experiments, such as the ^{13}C-HMQC (overall duration time T) and the ^{15}N-HMQC (overall duration time T'; $T' > T$) experiments, will spend a total collection time of $T + T'$, the TS approach would allow reduce the total acquisition time for a theoretical T time by collecting both data simultaneously.

To keep the simplicity and the overall duration of the original pulse sequence trains, the number of additional pulses and delays must be keep to a minimum. In practice, TS implementation needs some pulse timing readjustment because of different ^{13}C and ^{15}N evolution behavior. Careful inspection to the overall sensitivity ratios must be experimentally evaluated to justify the use of the single TS over the two separate pulse sequences. The only additional requirement to run TS experiments is a minimum triple-channel hardware configuration.

Figure 3 shows some basic building blocks to allow simultaneous evolution of two different frequencies in a given time period. The element 3A stands for the simultaneous evolution of the two different J(CH) and J(NH) coupling constants during a fixed period, as found in INEPT-like periods. The

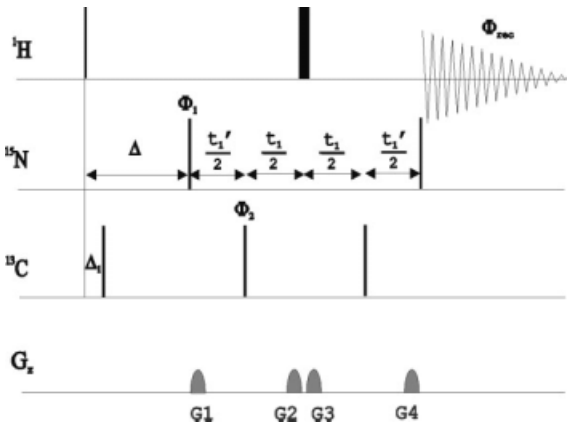

Figure 4 Pulse scheme of the TS-HMBC experiment for the simultaneous acquisition of ^{1}H/^{13}C-HMBC and ^{1}H/^{15}N-HMBC spectra. The Δ and Δ_1 delay are optimized to $1/2^n$J(XH) (6–8 Hz) and $1/2^1$J(CH) (145 Hz), respectively. Gradients G2 and G3 are optimized to select ^{13}C magnetization, whereas all four G1–G4 gradients select the equivalent ^{15}N coherence pathway (see Eqs. [1] and [2]) G1 = 60, G2 = 50, G3 = 30, and G4 = 60. Two different data are acquired and processed using the nucleus editing procedure schematically described in Fig. 5. In first data set $\phi_1 = x, -x$, $\phi_2 = x, -x$, and $\phi_{rec} = x, -x$. In second data set $\phi_1 = -x, x$, $\phi_2 = x, -x$, and $\phi_{rec} = x, -x$. Figure modified from Ref. *21*.

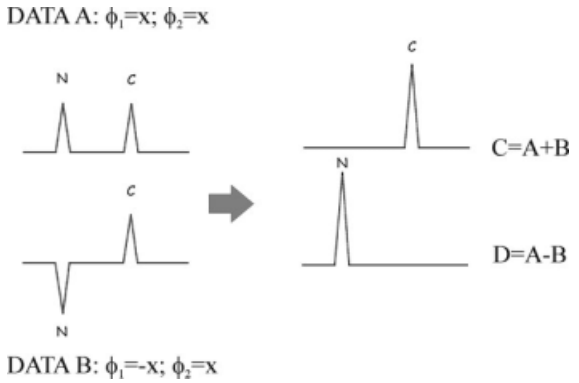

Figure 5 Data acquisition and data processing procedures to achieve nucleus editing in TS experiments. Two equivalent data (A and B) are separately collected in an interleaved mode with inversion of the phase ϕ_1 (see scheme of Fig. 3). After proper linear time-domain data combination, individual C and D spectra are obtained retaining maximum sensitivity.

evolution of the different sized J(CH) and J(NH) couplings can be individually optimized as a function of the Δ (=1/4*J(NH)) and Δ' (=1/4*J(CH)) delays. In the case of one-bond coupling constants evolution (^{1}J(CH) in the range of 130–160 Hz and ^{1}J(NH) about 90 Hz), carbon magnetization spent a little more time in the transverse plane than in the conventional single-frequency INEPT block. In practice, the additional ^{13}C relaxation during this extra ~2 ms period is not a serious inconvenient for small molecules. The element 3B stands for the simultaneous, but independent, ^{13}C and ^{15}N chemical shift evolution during an incremented t_1 (and t_1') period of a multidimensional experiment. Because spectral widths need to be independently optimized for the different ^{13}C and ^{15}N heteronuclei, Δt_1 and $\Delta t_1'$ are set to 1/SW(C) and 1/SW(N) − 1/SW(C), respectively. Other important experimental aspects such as the different number of t_1/t_1' increments or the required resolution in the indirect dimension for each individual heteronuclei will be discussed later.

Because ^{1}H bonded to ^{13}C is not bonded to ^{15}N, two independent coherence pathways are generated in TS experiments and they can be analyzed separately. In addition, the independence of these two evolutions during fixed or variable periods comes because at natural isotopic abundance is quiet improbably to find protons coupled both ^{13}C and ^{15}N (1.07 and 0.364% natural abundance). However, the evolution of homonuclear J(CC) and heteronuclear J(CN) coupling constants should be taken in account in ^{13}C/^{15}N isotopically enriched samples. In these cases, modified concatenated and constant-time periods should be incorporated in a similar way.

The resulting FID in TS experiments will contain both ^{1}H(^{13}C) and ^{1}H(^{15}N) data that can be easily differentiated by proper phase cycling and further simple data processing (*12*). We refer to this differentiation procedure as a nucleus editing in TS experiments. Experimentally, instead of recording a single TS experiment with 2N transients for each t_1/t_1' increment, two complementary data with a 180° phase difference between C and N coherence pathways (setting of the phases ϕ_1 and ϕ_2 in element 3B) are collected with N scans each one. The separate C and N subspectra are obtained after addition/subtraction data processing but retaining maximum sensitiv-

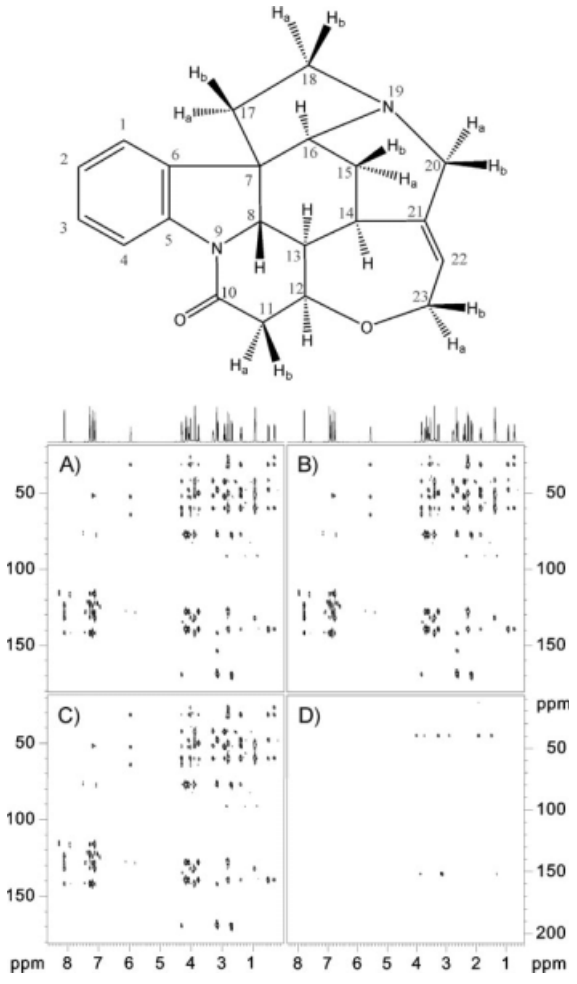

Figure 6 2D TS-HMBC spectra of strychnine obtained using the sequence of Fig. 4. Two data are separately acquired inverting the phase of ϕ_1 (A and B). Because of magnitude-mode presentation, these two different data cannot initially be differentiated. Linear combination and conventional data processing provide the separate C- and N-HMBC spectra, as shown in C and D. Experimental details of acquisition and processing are described in original Ref. *21*.

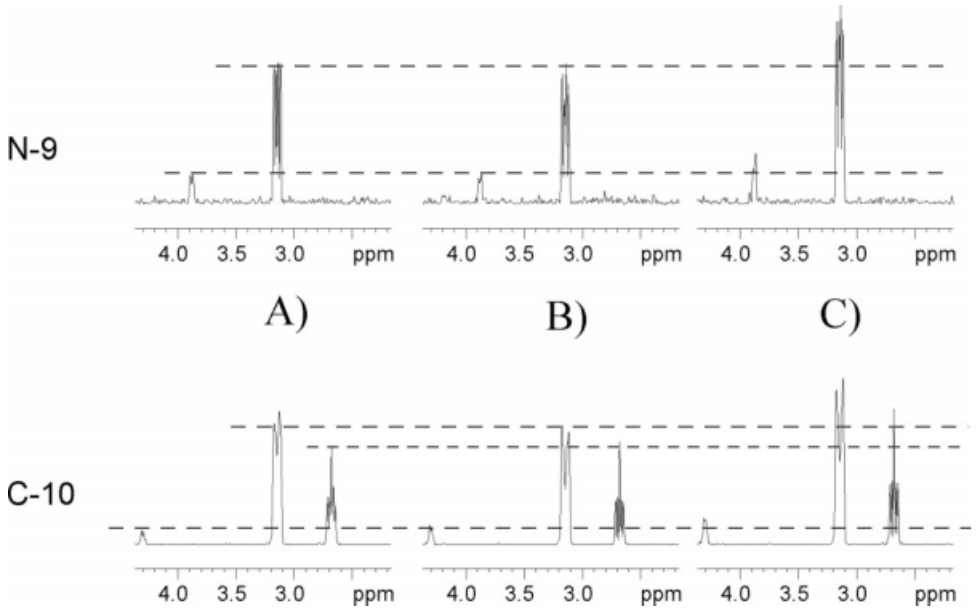

Figure 7 Experimental sensitivity gains achieved for the N9 and C10 in the TS-HMBC experiment of strychnine (see Fig. 6) when compared with the sequential acquisition of the regular C- and N-HMBC spectra. (A) Separate acquisition acquired with N transients for ^{13}C-HMBC and N transients for ^{15}N-HMBC (total experimental time = 2N), (B) TS-HMBC experiment acquired with N scans (total experimental time = N), and (C) TS-HMBC experiment acquiring two data with $\phi_1 = x$ (N scans) and $\phi_1 = -x$ (N scans) with a total acquisition time of 2N. Figure modified from Ref. *21*.

ity thanks to this Hadamard-like nucleus-edited encoding. Any NMR software package permits to perform the easy addition/subtraction protocol of time-domain data.

As in conventional inverse experiments, the position into the pulse sequence and the optimization of pulsed-field gradients play an important role. Both ^{1}H-^{12}C and ^{1}H-^{14}N magnetization components must be effectively removed by gradient coherence selection usually combined with a minimum two-step phase cycle. In practice, these gradients must be placed adequately to afford simultaneous coherence selection for ^{13}C and ^{15}N and, therefore, their positions can also introduce some minor changes into the pulse sequence timing.

TS-HMBC Experiment

The collection of ^{1}H/^{13}C-HMBC and ^{1}H/^{15}N-HMBC spectra is a very common and useful strategy for structural characterization of small- and medium-sized ^{15}N-containing compounds. We start the description of TS experiments by introducing the very important TS-HMBC experiment (Fig. 4) (*21*), which is closely related to the aforementioned TS-HMQC experiment (*13*). Here, the single evolution delay Δ is optimized to a single 6–8 Hz coupling value because both long-range ^{n}J(CH) and ^{n}J(NH) ($n > 1$) coupling constants present similar small values, in the range of 0–12 Hz. A low-pass J filter only for ^{13}C ($\Delta_1 = 1/2^{1}$J(CH)) is used to minimize direct correlation cross peaks but, optionally, higher low-pass ^{13}C filters and/or ^{15}N filters could also be incorporated. The number of pulses and the duration of the sequence are exactly the same as the regular ^{15}N-HMBC, and the major novelty is the additional length by a $+t_1'$ period when compared with the single ^{13}C-HMBC experiment. Pulsed-field gradients are strategically placed and optimized to simultaneously select both ^{13}C and ^{15}N coherence pathways. The general equations for optimal refocusing condition in the TS-HMBC pulse sequence are as follows:

$$\text{FOR } ^{13}\text{C: } (\gamma_H/\gamma_C) * G1 + (1 + (\gamma_H/\gamma_C)) * G2 + (1 - (\gamma_H/\gamma_C)) * G3 - (\gamma_H/\gamma_C) * G4 = 0 \quad [1]$$

$$\text{FOR } ^{15}\text{N: } (1 + (\gamma_H/\gamma_N)) * (G1 + G2) + (1 - (\gamma_H/\gamma_N)) * (G3 + G4) = 0. \quad [2]$$

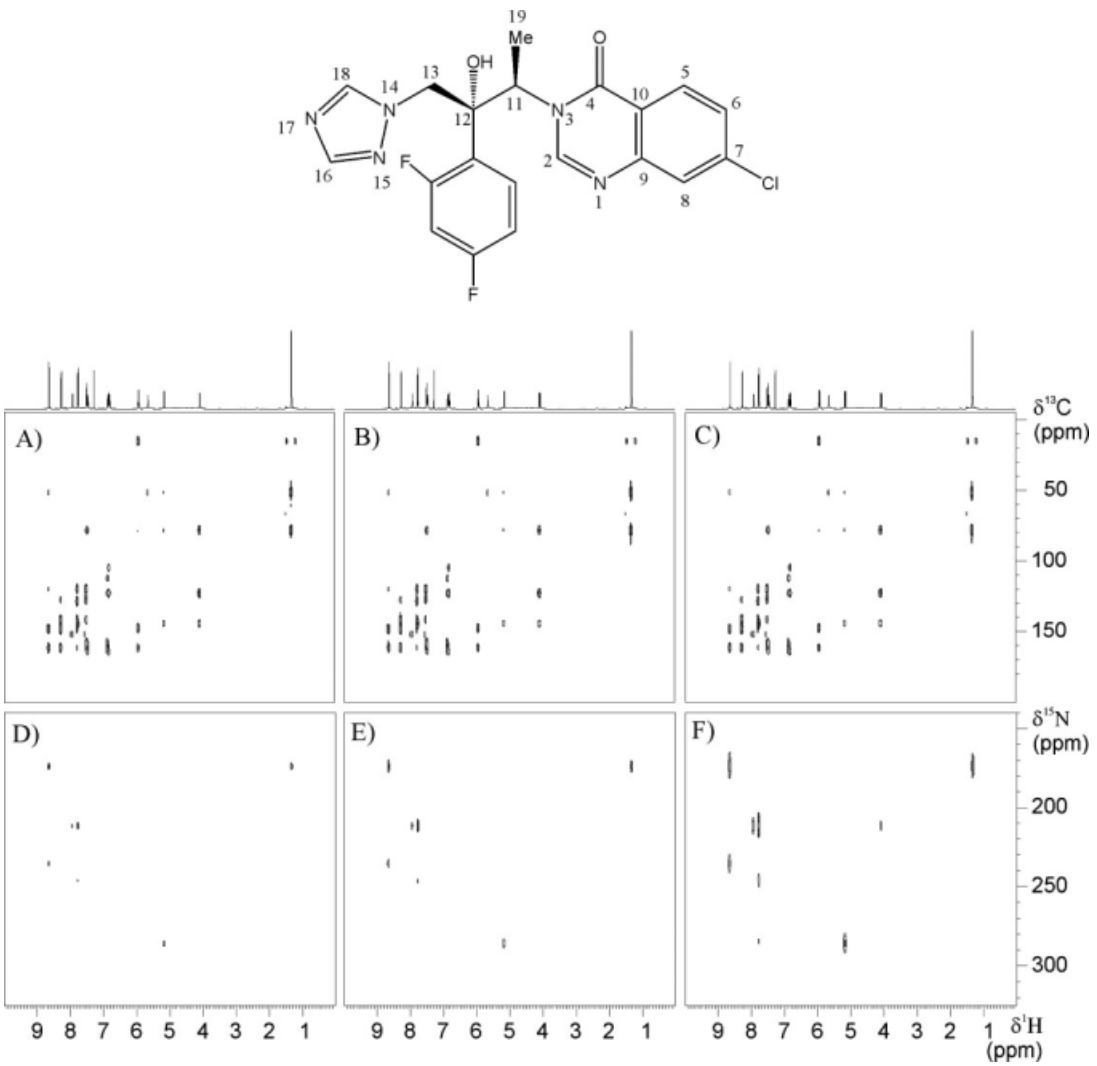

Figure 8 Individual optimization of spectral resolution for ^{13}C and ^{15}N nuclei in the indirect F1 dimension of the TS-HMBC experiment of albacanazole. The number of transients (NS) and the number of increments (NE) can be individually optimized for ^{13}C and ^{15}N as a function of a sensitivity k factor. D–F show the different resolution in the ^{15}N-HMBC spectra acquired with sensitivity factors of $k = 1$ (A and D), 2 (B and E), and 4 (C and F), respectively. Note that the resolution for ^{13}C in (A–C) is not affected. Experimental details can be found in Ref. *23*.

A relation 6:3:5:6 is a possible solution for both relationships. These equations are very important when applying the TS-HMBC experiment for other heteronuclei different to ^{13}C or ^{15}N.

When setting the TS-HMBC experiment, it is necessary to define the relative resolution needed between ^{13}C and ^{15}N in the indirect dimension. Thus, implementing a reduced ^{15}N spectral width (higher resolution) is done by increasing the $\Delta t_1'$ period, and this can imply ^{13}C sensitivity losses when compared with the standard experiment. Otherwise, implementing large ^{15}N spectral width (poorer resolution) is done using a shorter $\Delta t_1'$ period and, therefore, these ^{13}C sensitivity relaxation losses can be notably minimized. In practice, a compromise situation has to be chosen. A deeper discussion about optimizing sensitivity and resolution in TS experiments will be presented later.

Because of the magnitude-mode presentation, TS-HMBC experiment is best recorded with nucleus editing (Fig. 5). Two complementary data are acquired in an interleaved mode. The first experiment uses the same relative phase for ϕ_1 and ϕ_2 (Data A), whereas the second experiment inverts the phase

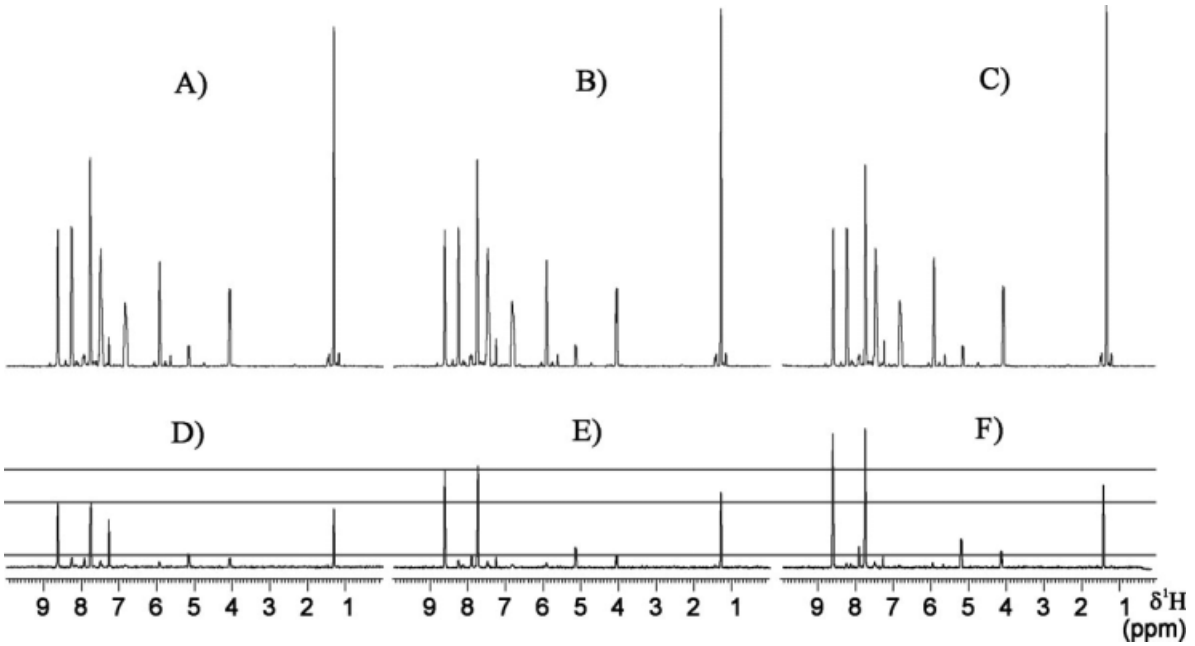

Figure 9 Sensitivity gains achieved for ^{15}N in the TS-HMBC experiment as a function of the sensitivity k factor, as shown in Fig. 8. Note that ^{13}C sensitivity is not affected (upper traces), whereas the sensitivity for ^{15}N can be increased by a 100% when comparing slices D ($k = 1$) vs. F ($k = 4$). Experimental details can be found in Ref. *23*.

ϕ_1 with respect to ϕ_2 (Data B). Time-domain addition (A + B) and subtraction (A − B) will afford the separate ^{13}C and ^{15}N spectra whereas retain maximum sensitivity. Figure 6 shows the resulting TS-HMBC spectra for the alkaloide strychnine. The relative sensitivity gains per time unit when running TS parallel acquisition vs. separate acquisition around square root of 2 (41%) predicted by theory are reached experimentally (Fig. 7).

The TS-HMBC experiment is a powerful tool for structural characterization of nitrogen-containing small molecules (*22*) and, in particular, it can be useful to

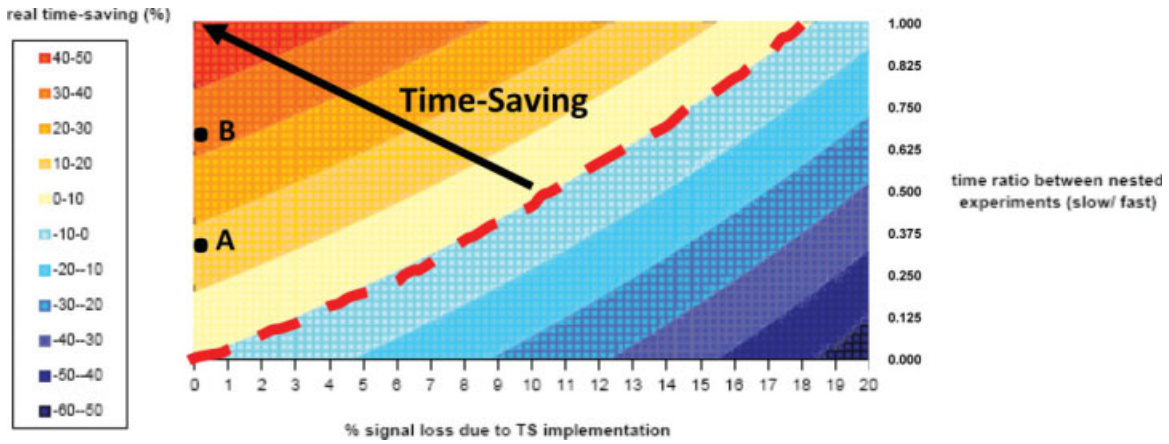

Figure 10 3D curve representation of the time saving in TS experiments as a function of % signal loss due to TS implementation and time ratio between combined experiments. Taking into account the sensitivity ratio between ^{15}N and ^{13}C nuclei (0.34), point A marks the 17% of real experimental time saving of the herein described TS-HMBC (*21*), TS-HQSC (*25*), TS-HSQC-TOCSY (*31*), and TS-HSQCMBC (*31*). Point B situates the 34% real experimental time saving for the optimized TS-HMBC experiment (*23*), where a k factor of 4 introduces a 100% of sensitivity gain for ^{15}N nuclei, therefore, increasing the $^{15}N/^{13}C$ sensitivity ratio up to 0.68. [Color figure can be viewed in the online issue, which is available at www.interscience.wiley.com.]

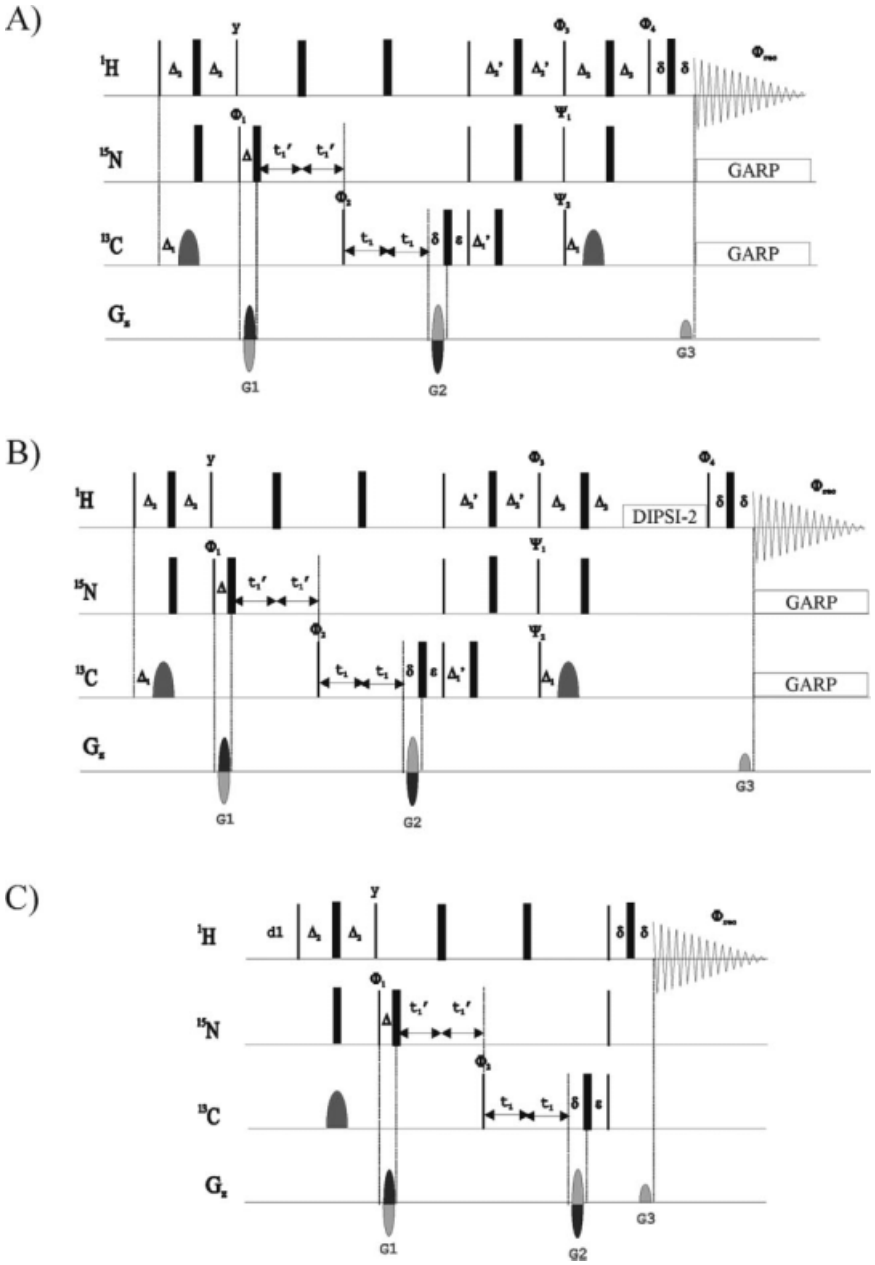

Figure 11 Time-shared versions of the HSQC-type pulse sequences: (A) TS-HSQC (*25*), (B) TS-HSQC-TOCSY (*31*), and (C) TS-HSQMBC experiments (*31*). Nucleus editing in all experiments can be achieved by proper setting of ϕ_1 and ϕ_2. IPAP editing in (A) and (B) can be achieved by proper setting of ϕ_3 and ϕ_4 as well as by omitting ^{13}C- and ^{15}N-decoupling during acquisition. All the necessary details (pulse phases, delays, and gradient strengths) for the practical implementation of the pulse sequences are described at original references.

obtain ^{15}N chemical shift values of nonprotonated nitrogens that can be highly difficult to be directly extracted from a very time-consuming 1D ^{15}N NMR spectrum. Many chemical features, such as N-oxidation, N-protonation, N-substitution patterns, tautomerism, and regiochemistry, can be studied from this experiment. TS-HMQC or/and TS-HMBC-related experiments can also be implemented between other spin 1/2 nuclei different than ^{13}C or ^{15}N, such as, for example, ^{29}Si, ^{31}P, ^{77}Se, or ^{119}Sn. Of course, those experiments might represent a big interest for the organometallic and inorganic chemistry community.

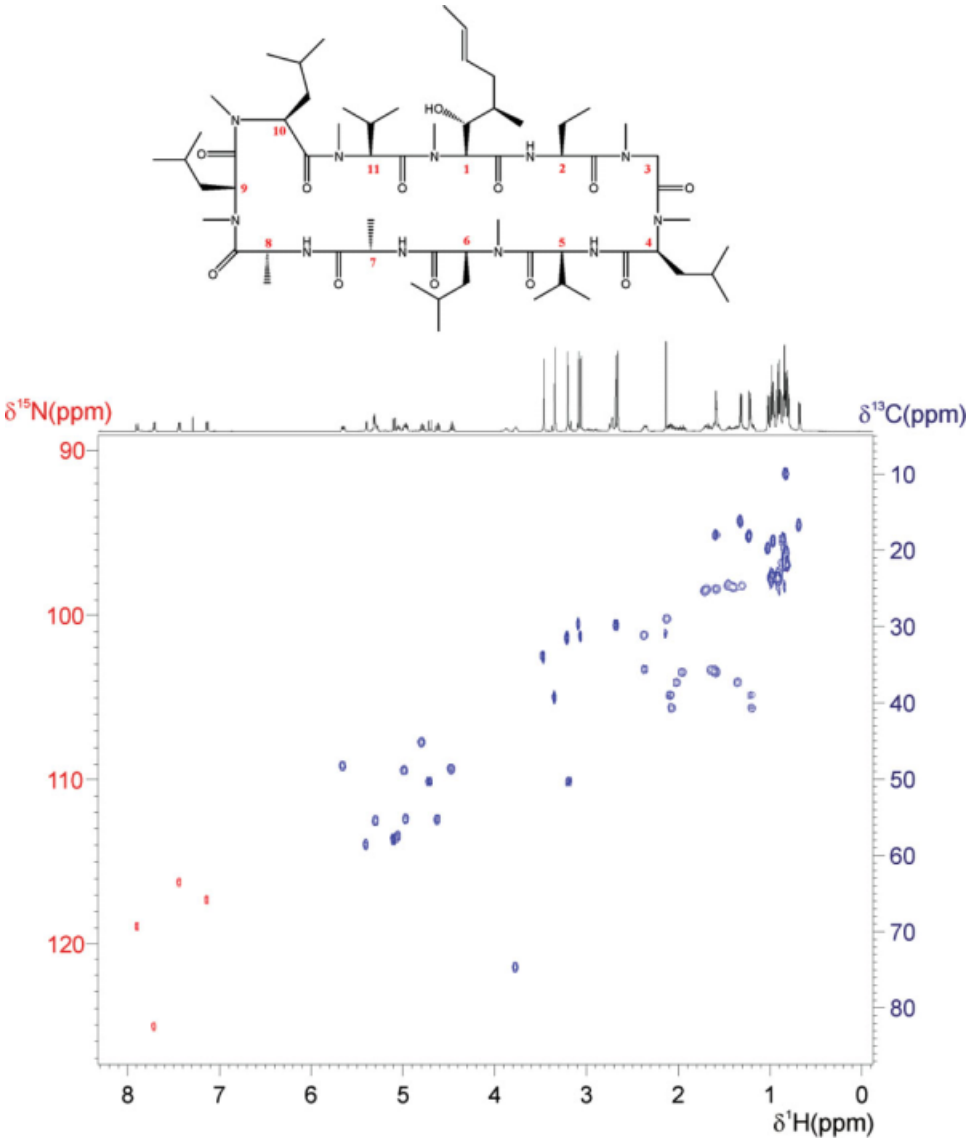

Figure 12 2D TS-HSQC spectra of cyclosporine acquired with the pulse sequence of Fig. 11(A) using pulse phases $\phi_1 = -x, x$, $\phi_2 = x, -x$, $\phi_3 = y$, $\phi_4 = x$, $\psi_1 = y$, $\psi_2 = y$, and $\phi_{rec} = x, -x$. Phase-sensitive representation allows to distinguish between ^{13}C (positive relative phase) and ^{15}N (negative relative phase) cross peaks. [Color figure can be viewed in the online issue, which is available at www.interscience.wiley.com.]

Optimizing Sensitivity and Resolution

One important topic when optimizing TS experiments is the relative sensitivity and resolution in the indirect dimension between the different heteronuclei. The natural abundance for ^{13}C and ^{15}N is 1.07 and 0.364%, respectively, that means that ^{13}C is 2.94 more sensitive than ^{15}N and, therefore, sensitivity limits in TS experiments will be mainly determined by ^{15}N. Another important point to take into account is the different spectral width and resolution required in the indirect dimension for each nucleus. Although a spectral width of ~220 ppm is usually enough to cover all ^{13}C-spectrum, the spectral width for ^{15}N can be more variable and undefined. Usually, spectral dispersion in ^{15}N is larger than ^{13}C, and a previous knowledge about the ^{15}N spectrum is not always available. On the other hand, molecules usually only have a few nitrogen centers and, therefore, resolution in the indirect F1 dimension for ^{15}N is not very criti-

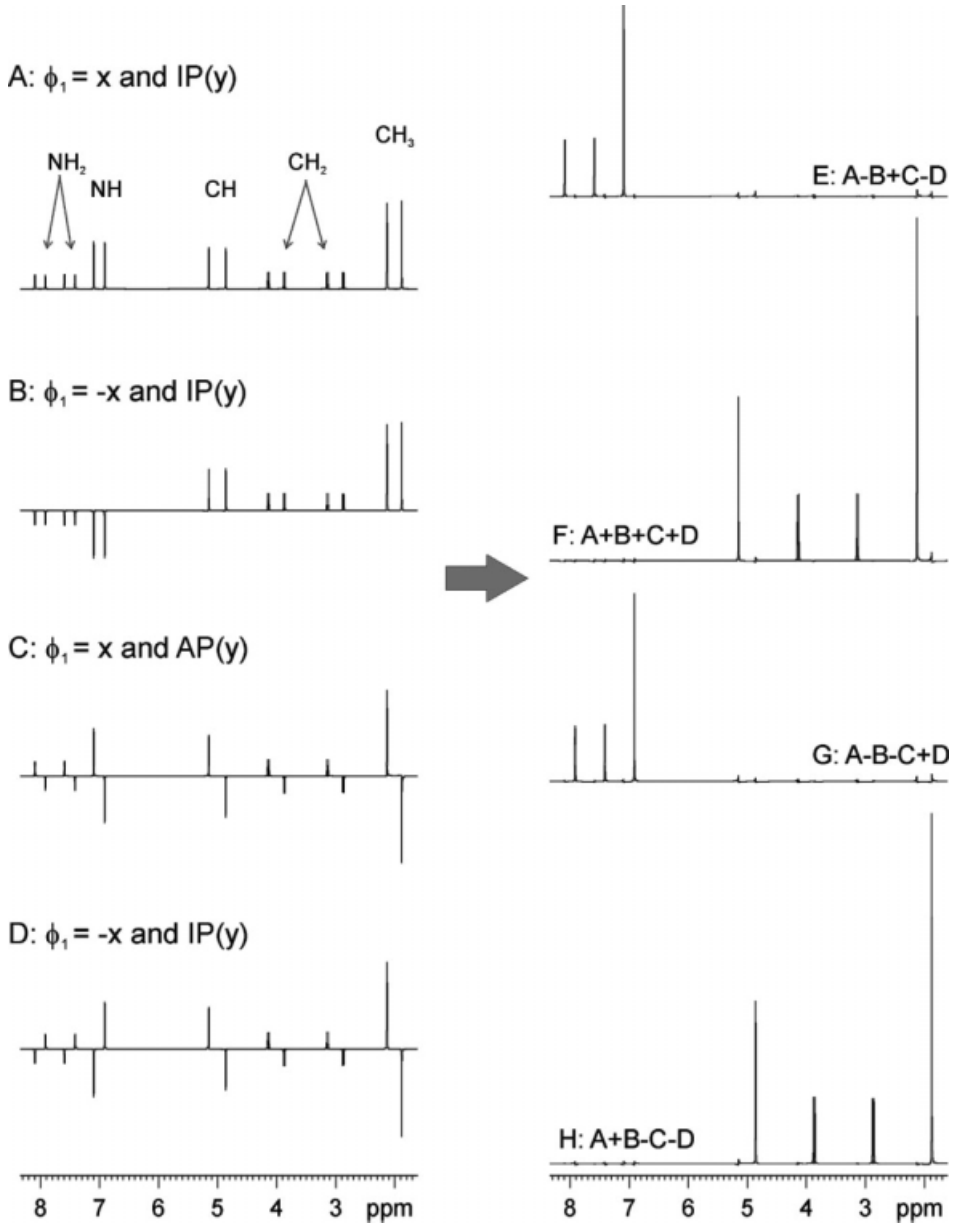

Figure 13 Simulation showing the nucleus and selective spin-state IPAP editing for all CH_n and NH_n multiplicities in the F2-IPAP TS-HSQC experiment. (E–H) Four separate line-selective NMR spectra are achieved after proper data combination. Full sensitivity is retained because all acquired (A–D) data contribute to the final signal. Figure modified from Ref. *25*.

cal. In summary, although ^{13}C needs more resolution than sensitivity, ^{15}N needs more sensitivity than resolution. An optimum and very simple solution should be to acquire less t_1/t_1' increments (NE) for ^{15}N but with increased number of transients (NS) without affecting the normal values for ^{13}C. This can be experimentally performed by incrementing the t_1 period each NE increments as usual, whereas the t_1' period is only incremented each k*NE increments. This is referred as the sensitivity k factor in TS experiments (*23*).

$$k = \mathrm{NS}(^{15}\mathrm{N})/\mathrm{NS}(^{13}\mathrm{C}) = \mathrm{NE}(^{13}\mathrm{C})/\mathrm{NE}(^{15}\mathrm{N}). \quad [3]$$

From the practical implementation point of view, the herein briefly explained optimized TS strategy is not trivial. A more detailed description is given in the original Ref. *23*. It is noteworthy that the pulse

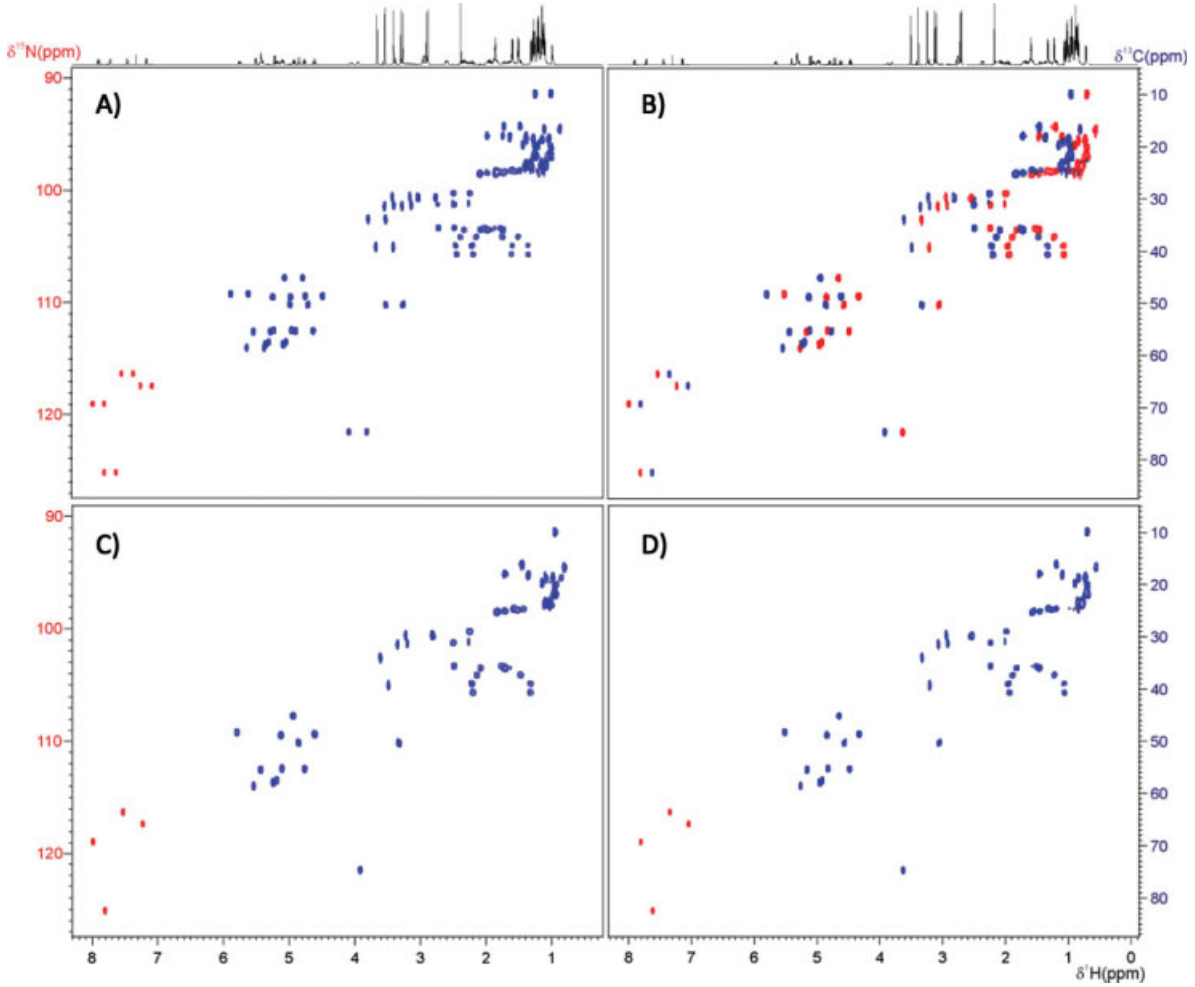

Figure 14 F2-IPAP TS-HSQC spectra of cyclosporine acquired as Fig. 12 but without heteronuclear decoupling during acquisition and including IPAP editing. (A) In-phase spectrum acquired using pulse phases $\phi_1 = -x, x$, $\phi_2 = x, -x$, $\phi_3 = y$, $\phi_4 = x$, $\psi_1 = y$, $\psi_2 = y$, and $\phi_{rec} = x, -x$. (B) Antiphase spectrum acquired using pulse phases $\phi_1 = -x, x$, $\phi_2 = x, -x$, $\phi_3 = x$, $\phi_4 = y$, $\psi_1 = y$, $\psi_2 = y$, and $\phi_{rec} = x, -x$. Linear combination A + B yield spectrum (C) α-spin state selection. Linear combination A − B yield spectrum (D) β-spin state selection. [Color figure can be viewed in the online issue, which is available at www.interscience.wiley.com.]

program code already incorporates the delay redefinition and the different data sampling and interleaved acquisition methods. On the other hand, a program written in C language automatically performs the convenient data management to afford the two separate spectra for rapid and direct interpretation: time-domain data addition followed by data subtraction and conventional processing to afford the ^{15}N spectrum after. Both pulse and automation programs are available for avance Bruker spectrometers upon request.

Figure 8 shows the resulting 2D TS-HMBC spectra of the drug albacanazole acquired with different sensitivity k factors but all under the same total acquisition time. In such 2D spectra, the resolution of ^{13}C data is not affected by the k factor, whereas ^{15}N resolution is coarse when increasing it. However, the five different nitrogen centers can easily be differentiated even for a k factor of 4 [Fig. 8(F)]. On the other hand, this loss of relative resolution is compensated by sensitivity enhancement of the less sensitivity of ^{15}N signal, as shown from the corresponding 1D slices shown in Fig. 9. In the case of the TS-HMBC experiment with $k = 4$ [compare Figs. 9(C, F) vs. 9(A, D)] the sensitivity is increased a 100% for ^{15}N, whereas ^{13}C is not affected.

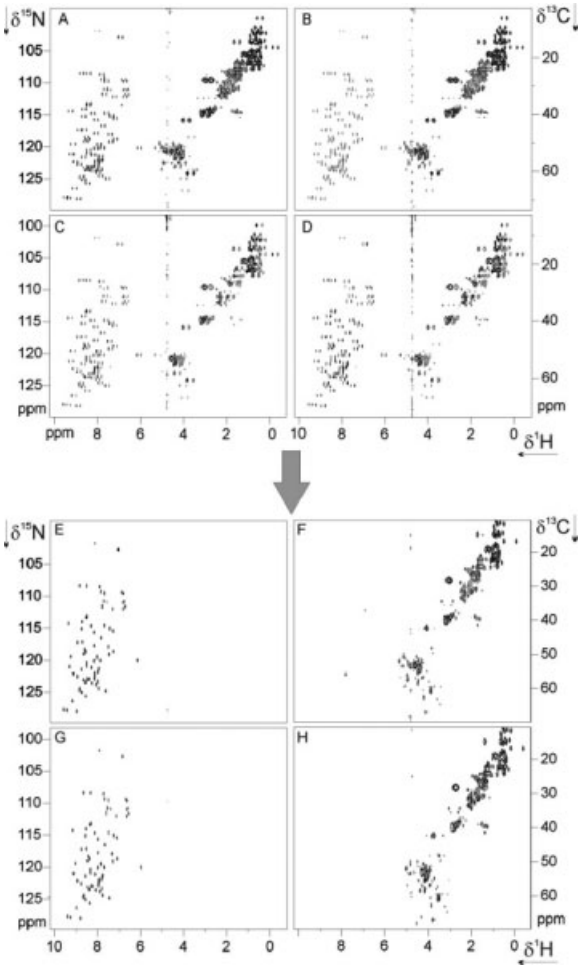

Figure 15 F2-IPAP TS-HSQC spectra of 1 mM ^{13}C,^{15}N-doubly labeled ubiquitine sample dissolved in 95% H_2O/5% D_2O. (A–D) Four different data are acquired with nucleus and IPAP editing. (E–H) Data combination affords four clean spectra with maximum sensitivity and better dispersion. Experimental details are described in the original publication (*33*).

Acceptable Sensitivity Loss in TS-Experiments

Combined TS experiments usually suffer from sensitivity losses mainly because of two factors, extra pulses and relaxation problems (because usually longer delays are required). It is important to highlight that severe loses in TS methodology can give rise to not really reach a real sensitivity gain with respect to the standard separate acquisition. For this reason when designing pulse sequences using TS strategy, it is of great importance to experimentally demonstrate the real gain per time unit comparing the signal-to-noise ratio of TS-experiments vs. standard ones, especially for the less sensitive nucleus. For example, if a X% of sensitivity lost is present in the less-sensitive experiment, then the TS experiment has to be run $(1 - X/100)^{-2}$ times the time for the regular experiment to recover the same signal-to noise ratio. Of course, redesign of the TS experiment will be needed if the required added time exceeds the time it would take to record the most sensitive experiment.

Another important factor that is not always well described when establishing the sensitivity gain in TS experiments is the relative sensitivity between the combined experiments. Theoretically, when combining two experiments in a TS fashion is possible to obtain up to 50% in time saving (41% in sensitivity gain). It is noteworthy that it is only really true when combining experiments with the same sensitivity or in other words with the same recording time. Usually that is not the case. For instance, recording a ^{15}N-HSQC is more time-consuming than recording a ^{13}C-HSQC (a factor of 2.94 according to its relative nucleus sensitivity). Taking into account the different sensitivity of combined experiments and sensitivity loss due to TS design, one can establish the real time saving using the following relationships (Fig. 10):

$$\text{Time Saving} = \text{Sensitivity factor}\,(\text{slow experiment}/\text{fast experiment}) - \text{TS loss Factor}\,(\text{slow experiment})$$

$$\text{Time Saving}(\%) = \left[\tfrac{1}{2}\,\text{slow experiment}/\text{fast experiment} - ((1 - \text{TSloss}(\%)/100)^{-2} - 1)\right] * 100.$$

It is noteworthy that all the TS approaches herein discussed (TS-HMBC, TS-HSQC, TS-HSQC-TOCSY, and TS-HSQMBC) have some sensitivity penalty for the most sensitivity experiment (^{13}C experiment). However, for the least sensitivity experiment (^{15}N experiment), there is almost no loss, because pulse sequences are designed with the same duration for that nucleus. The correct way to look at the real time gain is having in mind that while acquiring a 2D inverse ^{15}N spectrum is obtain the analogous ^{13}C experiment totally for free if using any of the TS experiments herein discussed, but that does not really represent a 50% of time saving because ^{13}C experiment is faster acquired than ^{15}N one. To calculate the real time saving is necessary to take into account the sensitivity ratio between ^{15}N and ^{13}C (0.34). Then, the theoretical maximum time saving is 17%. However, if a ^{15}N-sensitivity-optimized TS experiment using an optimum sensitivity k factor is recorded as

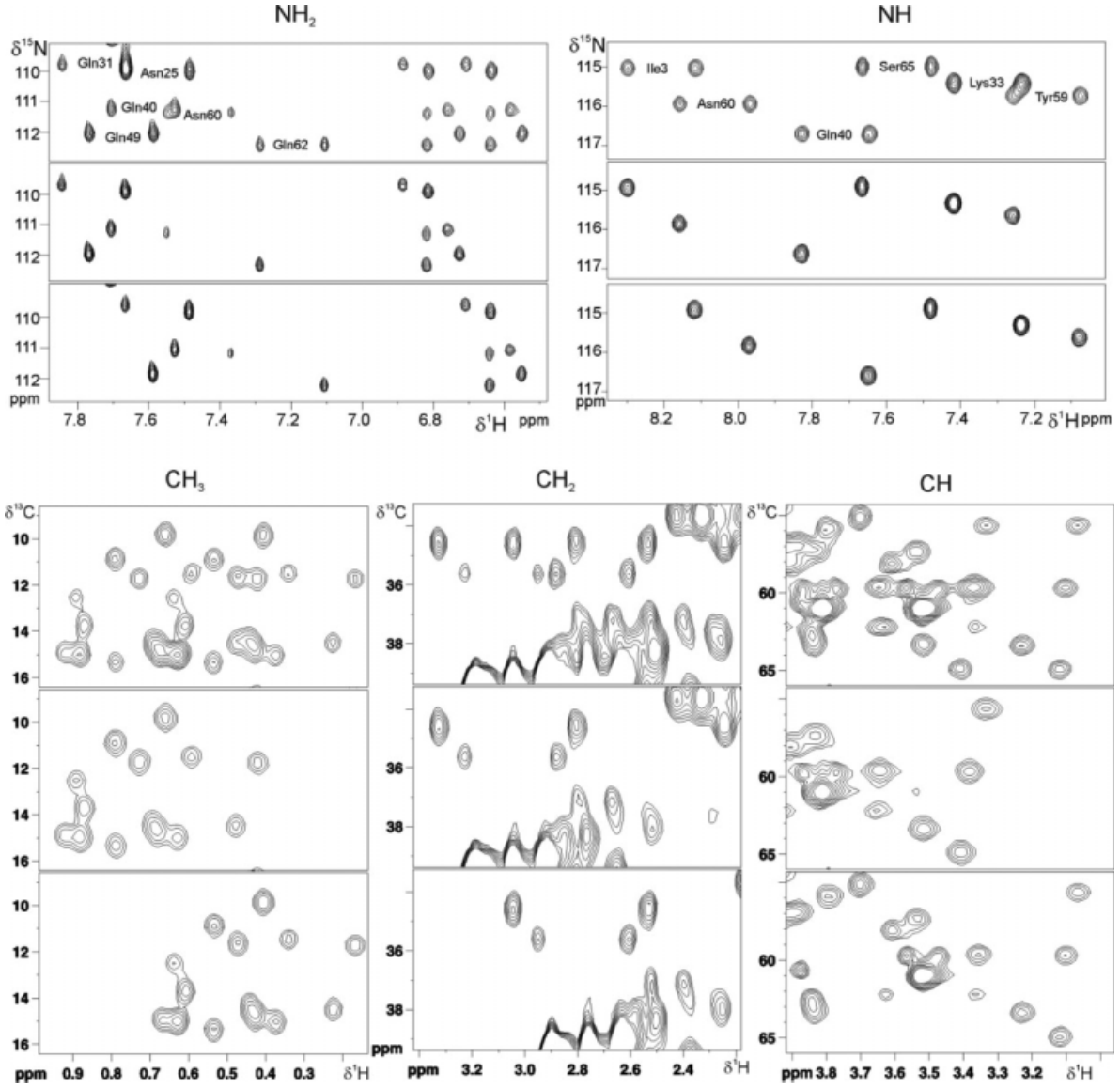

Figure 16 Expanded plots of the different edited HSQC spectra of Fig. 15. In each column, the top spectrum is the conventional in-phase experiment [corresponding to spectrum of Fig. 15(A)]; middle and bottom spectra are the two separate α/β-spectra [corresponding to spectra of Figs. 15(E–H)]. Note the excellent editing for all carbon and nitrogen multiplicities. Figure modified from Ref. *25*.

described in previous section is possible to increase the theoretical maximum time-saving factor. For instance, with a k factor of 4 is achieved a 100% of sensitivity gain for ^{15}N, which implies that the relative sensitivity ratio between ^{15}N and ^{13}C then becomes 0.68. Then, the theoretical maximum time-saving factor is 34%. As mentioned later, the TS approaches herein revisited do not suffer a signal loss in the ^{15}N spectrum. Thus, in these experiments, the experimental time saving is equal to the theoretically expected, 17% when standard implementation of TS is performed and 34% when using the optimized TS strategy.

TS-HSQC Experiment

Implementation of the TS principle into the HMQC pulse scheme would follow the same ideas described previously for the TS-HMBC experiment.

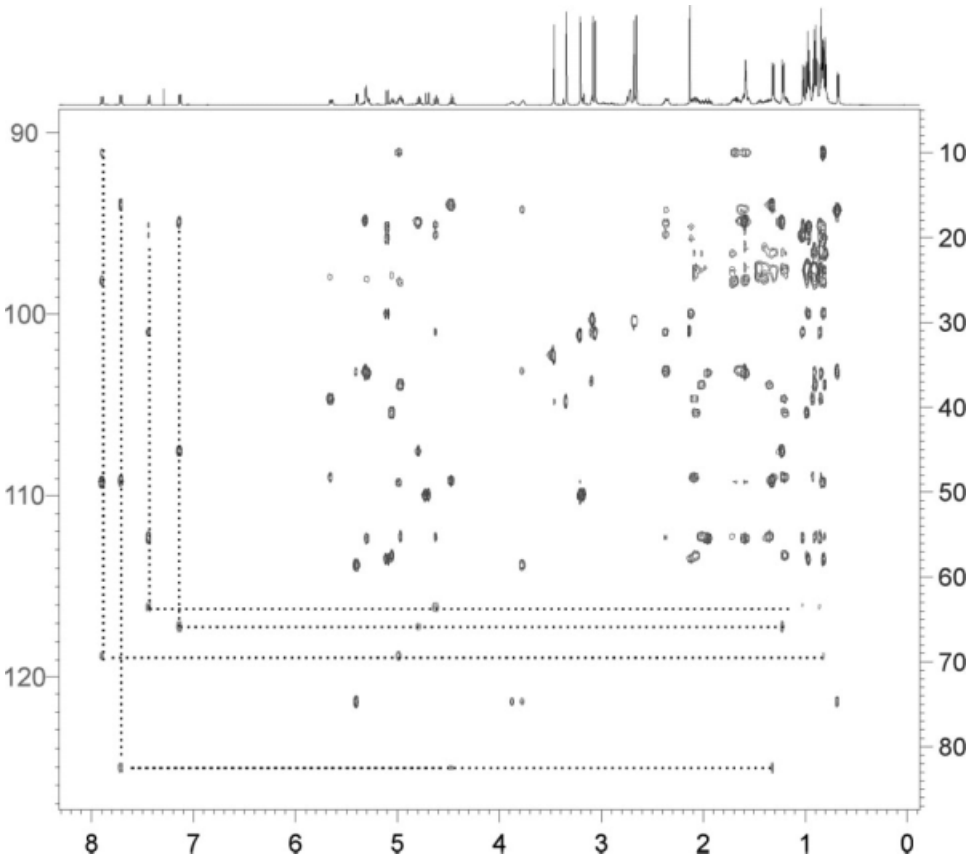

Figure 17 Experimental TS-HSQC-TOCSY of cyclosporine acquired with the pulse sequence of Fig. 11(B) with nucleus editing ($\phi_1 = -x$, x, $\phi_2 = x$, $-x$, $\phi_3 = y$, $\phi_4 = x$, $\psi_1 = y$, $\psi_2 = y$, and $\phi_{rec} = x$, $-x$). Phase-sensitive representation allows to distinguish between ^{13}C (positive relative phase) and ^{15}N (negative relative phase) cross peaks.

However, it can be more versatile and advantageous to perform one-bond heteronuclear correlations using the basic HSQC pulse scheme. Figure 11(A) shows the pulse scheme of the TS-HSQC experiment with gradient selection to obtain ^{1}H-^{13}C and ^{1}H-^{15}N HSQC spectra in the same 2D data set (*20*). As described previously, the typical INEPT blocks are substituted by concatenated heteronuclear echo steps to achieve simultaneous in-phase/antiphase J(CH) and J(NH) coupling evolution [see Fig. 3(A)]. On the other hand, ^{15}N magnetization is in the transverse plane during the variable t_1' and t_1 periods, whereas ^{13}C is present there only during the t_1 period. Thus, ^{13}C magnetization is stored as H_zC_z magnetization during the t_1' period. The TS-HSQC pulse sequence allows separate optimization of SW(C) and SW(N) as described previously and theoretically, a sensitivity gain of 41% per time unit should be achieved for both ^{13}C and ^{15}N. Experimentally, the major inconvenient arises for ^{13}C because longer echo times are required compared with the original ^{13}C HSQC (additional 2.2 ms for each heteronuclear echo) and the t_1' zz-filter should be maintained as short as possible. In practice, a compromise value between ^{13}C signal loss and required ^{15}N spectral resolution might be chosen. Nevertheless, it is important to highlight that the sensitivity of the TS experiment is governed by the lower NMR sensitivity found for ^{15}N compared with ^{13}C; therefore, a moderate loss of ^{13}C signal by relaxation is, a priori, not critical.

Figure 12 shows the TS-HSQC spectrum of the cyclopeptide cyclosporine in which ^{1}H, ^{13}C, and ^{15}N chemical shifts can be correlated and assigned in a single NMR spectrum. Because of the phase-sensitive data presentation in HSQC experiments, N- from C-cross peaks can be easily distinguished from their relative phase. In case of accidental resonance overlapping, the separate C- and N-HSQC spectra could be obtained by nucleus editing: interleaved data acquisition of two data [the same relative phase if $\phi_1 = \phi_2 = x$ but they have opposite phase if $\phi_1 = x$ and $\phi_2 = -x$ in Fig. 11(A)] and further time-domain data addition/subtraction.

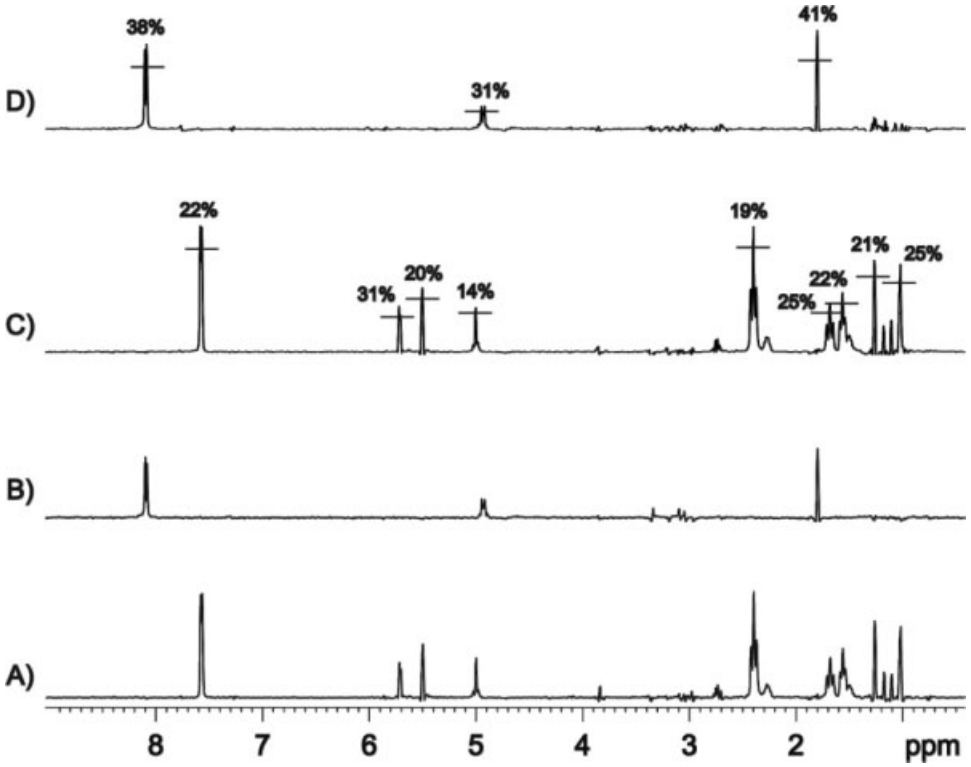

Figure 18 Experimental sensitivity gains obtained for the 2D TS-HSQC-TOCSY experiment of cyclosporine (C,D) when compared with the original ones (A,B). Although the expected gains about the theoretical 41% are reached for ^{15}N, averaged sensitivity gains around 20–30% are achieved for ^{13}C. Figure modified from Ref. *31*.

IPAP Editing in HSQC Experiments

Spin-state selective methodologies are nowadays widely extended in NMR spectroscopy, for instance, for measuring heteronuclear scalar and dipolar coupling constants or for selecting the most slowly relaxing component in proteins (TROSY selection). The same TS-HSQC scheme of Fig. 11(A) is well suited to obtain spin-state selection in the detected F2 dimension using the very simple IPAP approach described in Ref. *24*. Fully complementary in-phase (IP data: $\phi_3 = y$ and $\phi_4 = x$) and antiphase (AP data: $\phi_3 = x$ and $\phi_4 = y$) data are separately acquired without X-decoupling and further processed (IP $\pm$ AP) to obtain the individual α- and β-spectra. As demonstrated by theoretical simulations (Fig. 13), this F2-IPAP TS-HSQC experiment affords simultaneous α/β-editing for all CH, CH_2, CH_3, NH, and NH_2 multiplicities in the same spectra and with minimum crosstalks artifacts (*25*).

Figures 14(B,C) show the TS-HSQC-IP and TS-HSQC-AP spectra of cyclosporine, respectively. In the IP spectrum, positive NH cross peaks can be clearly distinguished from negative CH cross peaks. After combination of IP and AP data, α-edited and β-edited HSQC spectra are generated [Figs. 14(C,D)]. The TS-HSQC sequence offers excellent solvent suppression and, therefore, it can also be applied to large proteins dissolved in H_2O. In the TS-HSQC experiment of doubly-^{13}C, ^{15}N-labeled ubiquitine shown in Fig. 15, IPAP and nucleus editing have been combined to afford four individual spin-state selective HSQC-IPAP spectra. Note that the level of possible resonance overlapping in the conventional F2-coupled HSQC spectrum is strongly reduced in the four separate IPAP and nucleus-edited spectra [compare Figs. 15(A) vs. 15(E–H)]. Figure 16 shows spectra expanded regions visualizing the excellent spin-state selection achieved for all multiplicities.

Several modifications can be done to the TS-HSQC pulse sequence. For instance, it is possible to include a constant-time period to avoid evolution of homonuclear J(CC) during the variable t_1/t_1' periods

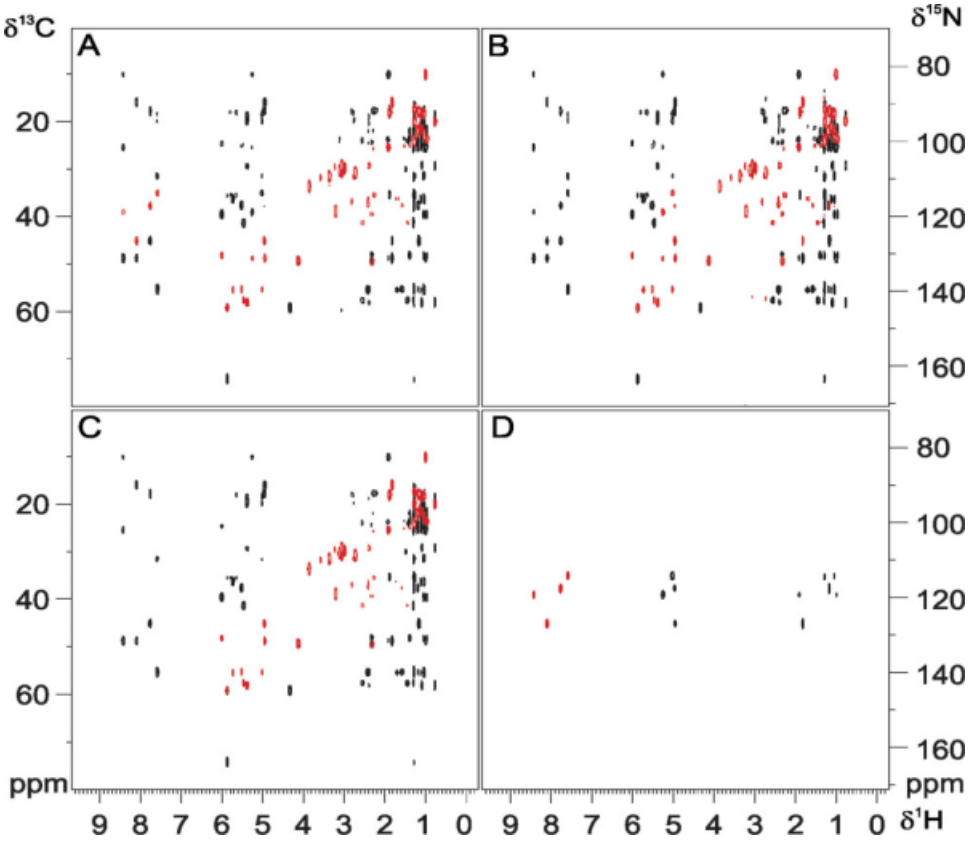

Figure 19 2D TS-HSQC-TOCSY spectra of cyclosporine incorporating direct-peak editing. The resulting individual spectra (C, D) obtained after postprocessing of A and B can distinguish direct HSQC from relayed TOCSY cross peaks for both C and N resonances in a single experiment. [Color figure can be viewed in the online issue, which is available at www.interscience.wiley.com.]

(*26*, *27*) in case of working with ^{13}C-labeled proteins. Also has been shown to be possible to achieve TROSY selection for ^{15}N nucleus while maintaining the standard decoupled HSQC cross peak for ^{13}C in large proteins (*28*, *29*). Alternatively, IPAP editing can also be achieved in the indirect dimension of the HSQC map (*30*). The resulting F1-IPAP TS-HSQC experiment (*25*) can take advantage of measuring both ^{1}J(CH) and ^{1}J(NH) coupling constants in the indirect F1 dimension, where there is no evolution of passive J(HH) coupling constants which is of maximum importance when measuring small RDC with high accuracy.

2D TS-HSQC-TOCSY Experiment

HSQC is the basis of many different 2D and higher dimensional NMR experiments, and therefore the properties described earlier can be extrapolated with high simplicity to a different number of other related applications. Figure 11(B) shows the basic scheme of the TS-HSQC-TOCSY experiment (*31*) in which the TOCSY building block (a DIPSI-2 pulse train) has been inserted before the beginning of the acquisition. This experiment provides complete and simultaneous ^{1}H, ^{13}C, and ^{15}N chemical shift residue assignment in peptides as shown for cyclosporine in Fig. 17. In this case, the relative sensitivity gains also reach the same levels as described earlier (Fig. 18).

TS-HSQC-TOCSY schemes can be used for multiple-purpose applications. For instance, editing of direct vs. relayed peaks can be applied to distinguish between direct HSQC and relayed TOCSY responses. This is made by replacing the last echo just before acquisition in the sequence of Fig. 11(B) for the building block sketched in Fig. 3(A). Figures 19(C, D) show the two complementary direct-edited ^{1}H/^{13}C and direct-edited ^{1}H-^{15}N HSQC-TOCSY spectra of cyclosporine.

It is also possible to simultaneously apply nucleus (ϕ_1 vs. ϕ_2) and IPAP (ϕ_3 and ϕ_4) editing in Fig.

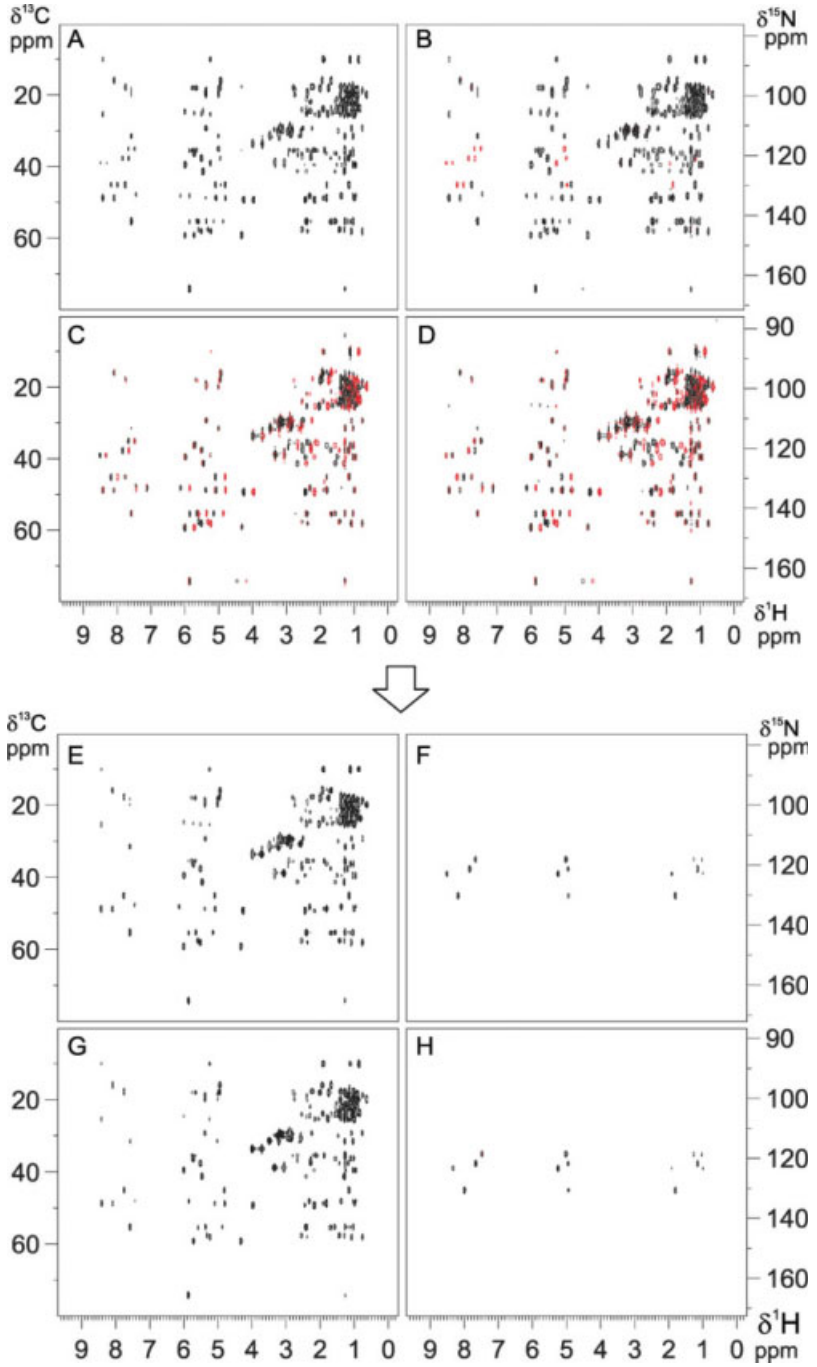

Figure 20 F2-IPAP TS-HSQC-TOCSY spectra of cyclosporine. Four individual spectra (E–H) are obtained retaining full sensitivity after nucleus and IPAP editing. Analysis of relative displacement of cross peaks afford simultaneous measuring of long-range J(CH) and J(NH) coupling constants, as described in Fig. 21. Experimental details can be found in the original publication (*31*). [Color figure can be viewed in the online issue, which is available at www.interscience.wiley.com.]

11(B), as described earlier for the TS-HSQC experiment. This 2D F2-IPAP TS-HSQC-TOCSY experiment afford line-selective α-C, β-C, α-N, and β-N spectra (Fig. 20) from which the easy, accurate, and simultaneous measurement of the sign and the magnitude of long-range ^{1}H-^{13}C and ^{1}H-^{15}N cou-

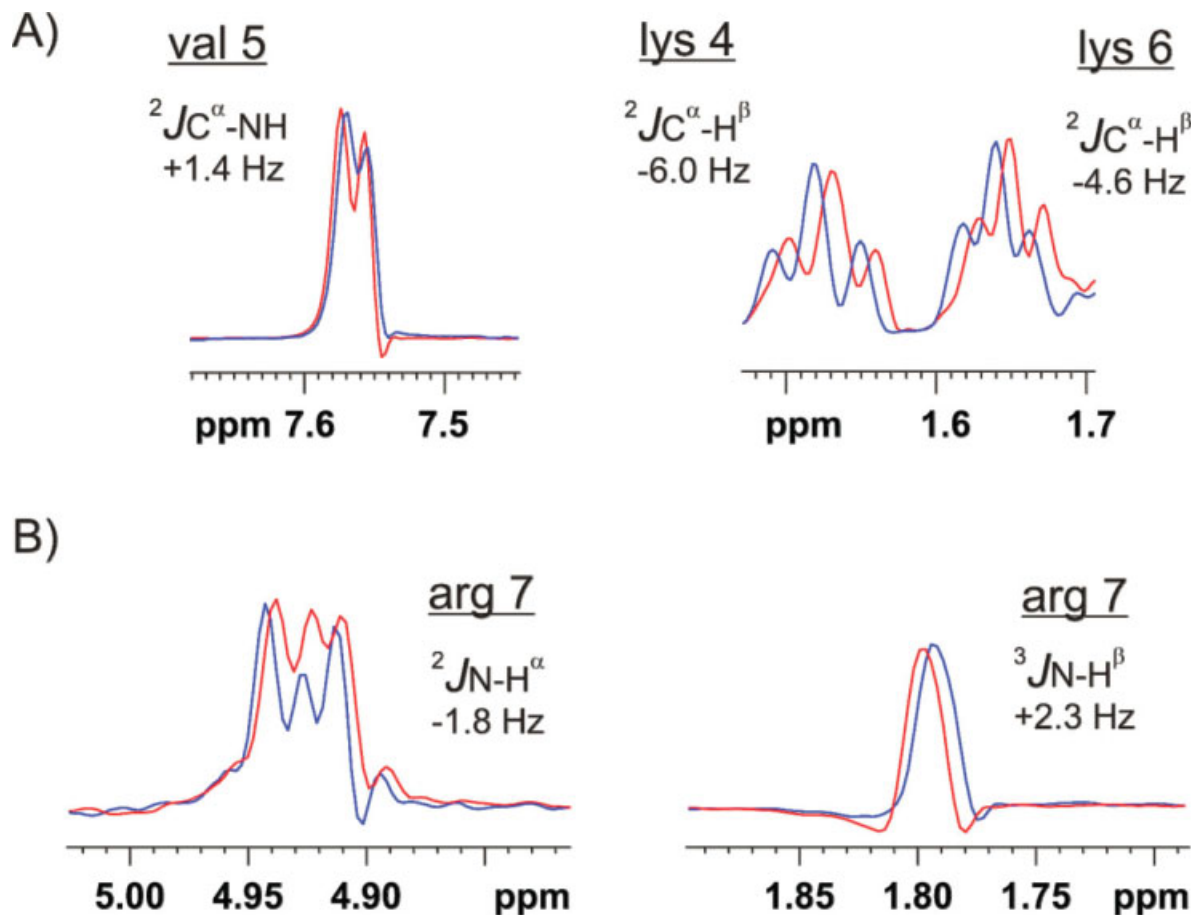

Figure 21 The sign and the magnitude of the ^nJ(CH) and ^nJ(NH) coupling constants for all protonated CH, CH_2, CH_3, NH, and NH_2 resonances are directly extracted for the relative displacement between cross peaks in edited HSQC-TOCSY spectra of Fig. 20. Figure modified from Ref. *31*. [Color figure can be viewed in the online issue, which is available at www.interscience.wiley.com.]

pling constants for all protonated ^{13}C and ^{15}N multiplicities can be performed. This is made by the direct analysis of the relative displacement of multiplet patterns in the corresponding 1D slice without any need for additional fitting procedure (Fig. 21). A good resolution in the acquisition dimension is strongly recommended.

2D TS-HSQMBC Experiment

The major drawback of HSQC-TOCSY-type experiments is that it fails for nonprotonated centers. Thus, the alternative to measure heteronuclear coupling constants on nonprotonated carbons and nitrogens must be phase-sensitive versions of the TS-HMBC or TS-HSQMBC experiments. The fundamentals of the former and its application to chemical shift assignments have also been discussed previously. The latter can easily be designed from the conventional TS-HSQC pulse sequence [Fig. 11(C)] by setting the interpulse delays to a single small value because the magnitudes of ^nJ(CH) and ^nJ(NH) have similar magnitudes and rarely exceeds 10 Hz. Thus, concatenated ^{13}C and ^{15}N periods are not needed. In addition, a minor number of pulses are involved because the refocusing retro-INEPT elements and X-decoupling for both ^{13}C and ^{15}N during the acquisition period are not applied. Thus, the TS-HSQMBC experiment allows the simultaneous acquisition of long-range ^1H-^{13}C and ^1H-^{15}N correlation spectra in absolute mode. The experiment works for all carbon multiplicities and therefore is a method of choice to measure such couplings in nonprotonated carbon and nitrogen centers. However, in contrast to HSQC-TOCSY-like spectra, a fitting procedure is necessary to analyze the anti-

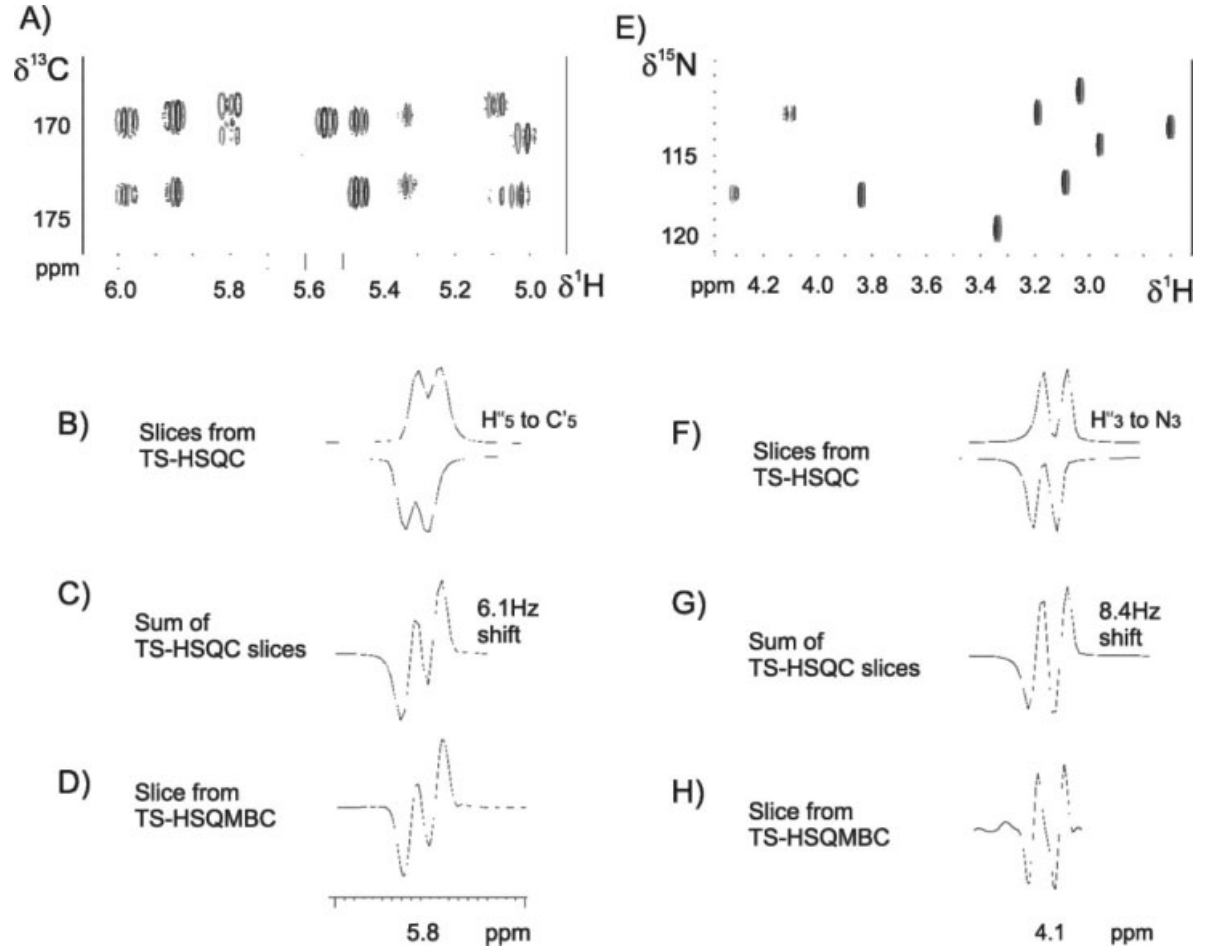

Figure 22 (A–E) Expansion plots extracted of the carbonyl and N-methyl region of the each TS-HSQMBC spectra of cyclosporine acquired using sequence of Fig. 11(C). All cross peaks show the characteristic antiphase cross pattern (see D and H) that must be analyzed using a proper fitting procedure (see for instance B/C and F/G). Experimental details are described in the original publication (*31*).

phase coupling patterns and to accurately determine long-range ^{n}J(XH) coupling constants values. 2D expansions of the CO and NMe regions of the TS-HSQMBC spectra of cyclosporine are shown in Fig. 22. As other TS experiments, sensitivity gains around 30–40% for both ^{13}C and ^{15}N are experimentally achieved when compared with the separate data acquisition, as theoretically predicted. More elaborated HMBC and HSQMBC sequences than presented here could be designed as, for instance, to remove undesired J(HH) modulation during the INEPT blocks by introducing CPMG pulse trains (*32*).

Miscellaneous TS Applications

The advantages of TS experiments can be combined with those of other independent accelerated NMR methods. For instance, it has been reported that TS experiments can be combined with the multiple-FIDs acquisition within the same scan approach (referred as MATS technique) to perform simultaneous acquisition of multiple and complementary NMR spectra (*33*) and, therefore, offering important spectrometer time savings. Figure 23 shows the basic pulse scheme of the MATS-HMBC experiment that is useful to record simultaneously 2D ^{1}H,^{13}C HMBC, ^{1}H,^{15}N HMBC, ^{1}H,^{13}C HMBC-COSY, and ^{1}H,^{15}N HMBC-COSY spectra, as shown in Fig. 24. Concerted analysis of all these spectra can give more information about two-, three- and four-bond away ^{1}H-^{13}C and ^{1}H-^{15}N connectivities.

TS techniques can also found interesting applications when multiple channels or multiple receiver coils will be available. For instance, TS would provide simultaneous acquisition of ^{1}H,^{13}C-HMBC,

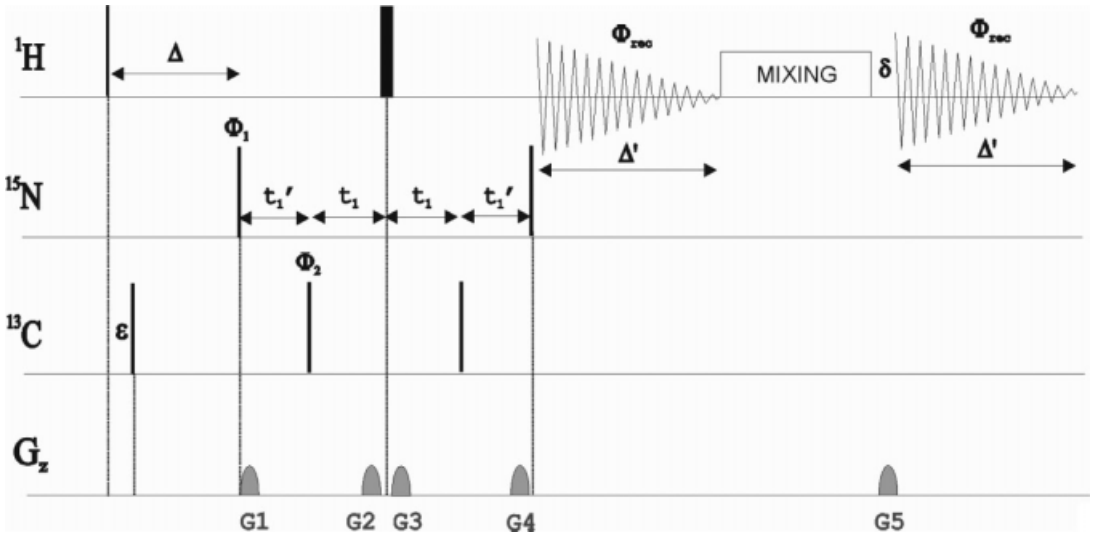

Figure 23 General pulse scheme of the MATS-HMBC experiment, including a second FID acquisition within the same scan. The mixing box can stand for COSY or TOCSY blocks. Data are stored in separate memory blocks and four spectra can be obtained simultaneously with full sensitivity ratios after conventional processing. Experimental details are described in the original Ref. *33*.

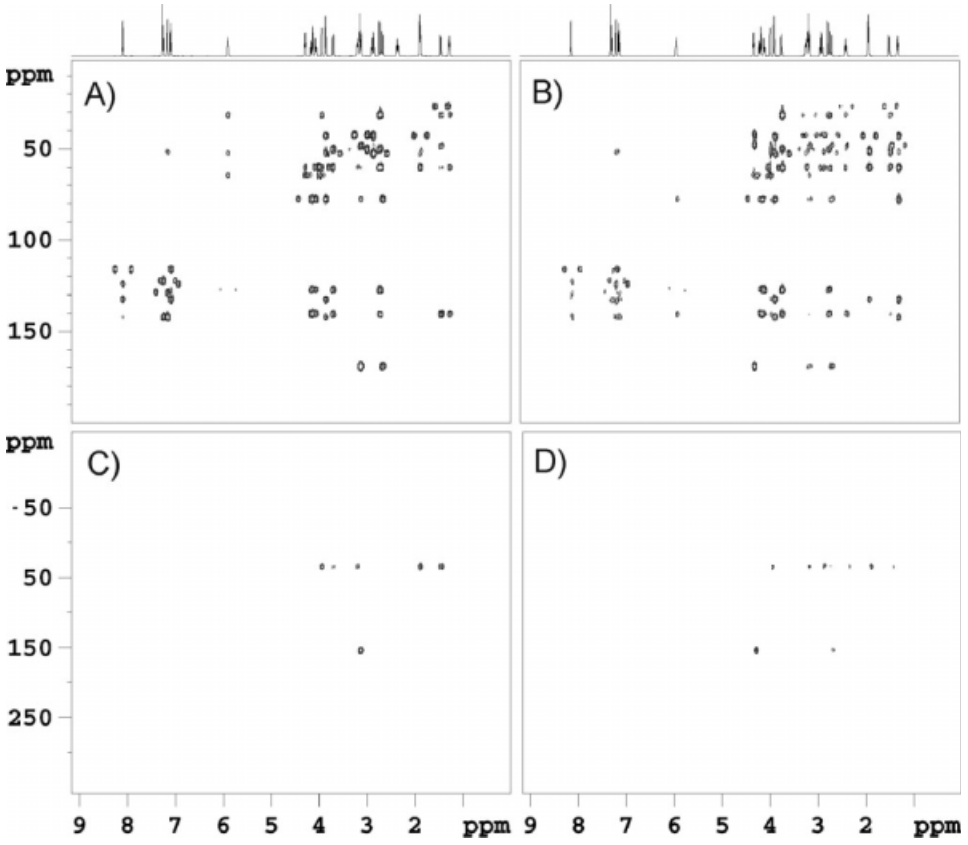

Figure 24 Individual 2D ^{1}H/^{13}C HMBC, ^{1}H/^{13}C HMBC-COSY, ^{1}H/^{15}N HMBC, and ^{1}H/^{15}N HMBC-COSY spectra of strychnine simultaneously obtained from a single-shot acquistion of the MATS-HMBC experiment. Each spectrum provides different but complimentary information. Experimental details are described in the original publication (*33*).

$^{1}H,^{15}N$-HMBC, and $^{1}H,^{31}P$-HMBC spectra if a four-channel hardware configuration is available. Also interesting is the use of parallel acquisition when multiple detection coils can be available. Recently, a series of experiments under the acronym PANSY (parallel acquisition NMR spectroscopy) have been proposed allowing the simultaneous acquisition of different nuclei in the detected dimension. It has been demonstrated its usefulness with the simultaneous acquisition of proton-detected and fluorine-detected HMBC spectra (*34*, *35*).

TS experiments can also be successfully combined with projection-reconstruction (*36*) techniques as recently reported to obtain a forbidden $^{13}C/^{15}N$ correlation map at natural abundance from a TS-HMBC experiment. TS techniques have also been combined with GFT taking the accumulative advantage of these two speed-up methodologies. Specifically, the GFT-TS combination has been proven to be of utility in the acquisition of 4D NOESY experiments in small- to medium-sized proteins (*37*). In fact, TS experiments have been traditionally proposed as a useful alternatives to the time-consuming 3D and 4D NOESY-HSQC experiments to detect NOEs from backbone and side-chain protons in doubly labeled proteins to reduce conveniently the very large acquisition times (*38–41*). In addition, several applications have also been reported for the simultaneous measurement of scalar or dipolar coupling constants for backbone NH and side-chain CH, CH_2, and CH_3 spins systems (*26*), to monitor chemical shift changes using the SAR by NMR principles simultaneously for NH and CH_3 (*42*), for the simultaneous acquisition of HNCO and HNCA spectra in ^{15}N-labeled proteins (*43*) or for the simultaneous evolution of different coherences in multidimensional experiments of labeled proteins, as reported for chemical shift assignment of HA, HN, CA, and N from 3D TS-(HN)NCAHA and (HA)CANNH experiments (*44*). Conceptually, this resembles to the RD approach, based on the acquisition of lower dimension experiments instead of time-consuming high-dimension experiment.

Although this is not a highly critical point, the reader must remind that the high rf power produced during simultaneous 15N/13C-decoupling in the acquisition period could be a potential danger for the probe head.

CONCLUSIONS

In this article, we have described how multiple spectra can be obtained from a single NMR experiment using the TS multiple-frequency evolution concept. The main advantages are spectrometer time savings and multiple data collection from a single-shot acquisition. It has been demonstrated that with the time needed to obtain a ^{15}N spectrum, the equivalent ^{13}C spectrum is freely obtained. This parallel acquisition method can afford sensitivity enhancements up to 41% or time savings up to 50% when compared with the classical sequential data acquisition protocol. As conventional experiments, all TS experiments implementation permit an easy, automated set-up, and routine use using conventional processing and general applicability. In practice, the major sensitivity limitations are the same as found in conventional ^{15}N experiments data collection although they can be applied on any pair of active spin-1/2 nuclei other than ^{13}C and ^{15}N. The flexibility of the TS approach allows to be combined with other fast NMR methods allowing simultaneous acquisition of multiple complementary spectra and improving data collection time. The TS method can have high interest in future developments with multiple receiver coil systems.

ACKNOWLEDGMENTS

This work was supported by MCYT (project CTQ2006-01080, CTQ2009-08328, and Consolider Ingenio-2010 CSD2007-00006). The authors are grateful to the Servei de Ressonància Magnètica Nuclear, UAB, for allocating instrument time to this project.

REFERENCES

1. Parella T. 1998. Pulsed-field gradients: a new tool for routine NMR. Magn Reson Chem 36:467–495.
2. Sattler M, Schleucher J, Griesinger C. 1999. Heteronuclear multidimensional NMR experiments for the structure determination of proteins in solution employing pulsed field gradients. Prog Nucl Magn Reson Spectrosc 34:93–158.
3. Atreya HS, Szyperski T. 2005. Rapid NMR data collection. Methods Enzymol 394:78–108.
4. Ross A, Salzmann M, Senn H. 1997. Fast-HMQC using Ernst angle pulse: an efficient tool for screening of ligand binding to target proteins. J Biomol NMR 10:389–396.
5. Kupce E, Nishida T, Freeman R. 2003. Hadamard NMR spectroscopy. Prog Nucl Magn Reson Spectrosc 42:95–122.
6. Kim S, Szyperski T. 2003. GFT NMR, a new approach to rapidly obtain precise high-dimensional NMR spectral information. J Am Chem Soc 125: 1385–1393.

7. Kupce E, Freeman R. 2003. Projection-reconstruction of three-dimensional NMR spectra. J Am Chem Soc 125:13958–13959.
8. Bobli M, Stern AS, Hoch JC. 2006. Spectral reconstruction method in fast NMR: reduced dimensionality, random sampling and maximum entropy. J Magn Reson 182:96–105
9. Frydman L, Scherf T, Lupulescu A. 2002. The acquisition of multidimensional NMR spectra within a single scan. Proc Natl Acad Sci USA 99:15858–15862.
10. Gal M, Schanda P, Brutscher B, Frydman L. 2007. UltraSOFAST HQMC NMR and the repetitive acquisition of 2D protein spectra at Hz rates. J Am Chem Soc 129:1372–1377.
11. Schanda P, Brutscher B. 2006. Hadamard frequency-encoded SOFAST-HMQC for ultrafast two-dimensional protein NMR. J Magn Reson 178:334–339.
12. Sørensen OW. 1990. Aspects and prospects of multidimensional time-domain spectroscopy. J Magn Reson 89:210–216.
13. Farmer BT II. 1991. Simultaneous [^{13}C,^{15}N]-HMQC, a pseudo-triple-resonance experiment. J Magn Reson 93:635–641.
14. Burgering M, Boelens R, Kaptein R. 1993. Observation of inter-subunit NOEs in a dimeric P22 MNT repressor mutant by a time-shared (^{13}C, ^{15}N) double half-filter technique. J Biomol NMR 3:709–714.
15. Boelens R, Burgering M, Fogh RH, Kaptein R. 1994. Time-saving methods for heteronuclear multidimensional NMR of (^{13}C, ^{15}N) doubly labelled proteins. J Biomol NMR 4:201–213.
16. Farmer BT, Mueller L. 1994. Simultaneous acquisition of [^{13}C, ^{15}N]- and [^{15}N, ^{15}N]-separated 4D gradient-enhanced NOESY spectra in proteins. J Biomol NMR 4:673–687.
17. Kay LE, Wittekind M, McCoy MA, Friedrichs MS, Mueller L. 1992. 4D NMR triple-resonance-experiments for protein backbone nuclei using shared constant-time evolution periods. J Magn Reson 98:443–450.
18. Mariani M, Tessari M, Boelens R, Vis H, Kaptein R. 1994. Assignment of the protein backbone from a single 3D ^{15}N,^{13}C, time-shared HXYH experiment. J Magn Reson B 104:294–297.
19. Pascal SM, Muhandiram DR, Yamazaki T, Forman-Kay JD, Kay LE. 1994. Simultaneous acquisition of ^{15}N- and ^{13}C-edited NOE spectra of proteins dissolved in H2O. J Magn Reson B 103:197–201.
20. Sattler M, Maurer M, Schleucher J, Griesinger C. 1995. A simultaneous ^{15}N, ^{1}H-HSQC and ^{13}C, ^{1}H-HSQC with sensitivity enhancement and a heteronuclear gradient-echo. J Biomol NMR 5:97–102.
21. Pérez-Trujillo M, Nolis P, Parella T. 2007. CN-HMBC: a powerful NMR technique for the simultaneous detection of long-range H,C and H,N connectivities. Org Lett 9:29–32.
22. Martin GE, Hadden CE. 2000. Long-range H-N heteronuclear shift correlation at natural abundance. J Nat Prod 63:543–585.
23. Pérez-Trujillo M, Nolis P, Bermel W, Parella T. 2007. Optimizing sensitivity and resolution in time-shared NMR experiments. Magn Reson Chem 45: 325–329.
24. Nolis P, Espinosa JF, Parella T. 2006. Optimum spin-state selection for all multiplicities in the acquisition dimension of the HSQC experiment. J Magn Reson 180:39–50.
25. Nolis P, Parella T. 2007. Simultaneous alpha/beta spin-state selection for ^{13}C and ^{15}N from a time-shared HSQC-IPAP experiment. J Biomol NMR 37: 65–77.
26. Wurtz P, Permi P. 2007. SESAME-HSQC for simultaneous measurement of NH and CH scalar and residual dipolar couplings. Magn Reson Chem 45:289–295.
27. Uhrin D, Bramham J, Winder SJ, Barlow PN. 2000. Simultaneous CT-^{13}C and VT-^{15}N chemical shift labelling: application to 3D NOESY-CH3NH and 3D ^{13}C, ^{15}N HSQC-NOESY-CH_3NH. J Biomol NMR 18: 253–259.
28. Pervushin K, Braun D, Fernandez C, Wuthrich K. 2000. [^{15}N,^{1}H]/[^{13}C,^{1}H]-TROSY for simultaneous detection of backbone ^{15}N-^{1}H, aromatic ^{13}C-^{1}H and side-chain ^{15}N-^{1}H-1(2) correlations in large proteins. J Biomol NMR 17:195–202.
29. Guo C, Tugarinov V. 2009. Identification of HN-methyl NOEs in large proteins using simultaneous amide-methyl TROSY-based detection. J Biomol NMR 43:21–30.
30. Ottiger M, Delaglio F, Bax A. 1998. Measurement of J and dipolar couplings from simplified two-dimensional NMR spectra. J Magn Reson 131:373–378.
31. Nolis P, Pérez M, Parella T. 2006. Time-sharing evolution and sensitivity enhancements in 2D HSQC-TOCSY and HSQMBC experiments. Magn Reson Chem 44:1031–1036.
32. Marquez BL, Gerwick WH, Williamson RT. 2001. Survey of NMR experiments for the determination of nJ(CH) heteronuclear coupling constants in small molecules. Magn Reson Chem 39:499–530.
33. Nolis P, Pérez-Trujillo M, Parella T. 2007. Multiple FID acquisition of complementary HMBC data. Angew Chem Int Ed 46:7495–7497.
34. Kupce E, Freeman R. 2006. Parallel acquisition of two-dimensional NMR spectra of several nuclear species. J Am Chem Soc 128:9606–9607.
35. Kupce E, Cheatham S, Freeman R. 2007. Two-dimensional spectroscopy with parallel acquisition of ^{1}H-X and ^{19}F-X correlations. Magn Reson Chem 45:378–380.
36. Kupce E, Freeman R. 2007. Natural-abundance ^{15}N-^{13}C correlation spectra of vitamin B-12. Magn Reson Chem 45:103–105.
37. Xia Y, Veeraraghavan S, Zhu Q, Gao X. 2009. Fast (4,3)D GFT-TS NMR for NOESY of small to medium-sized proteins. J Magn Reson 190:142–148.
38. Frueh DP, Vosburg DA, Walsh CT, Wagner G. 2006. Determination of all NOes in ^{1}H-^{13}C-Me-ILV-

U-^{2}H-^{15}N proteins with two time-shared experiments. J Biomol NMR 34:31–40.
39. Jerala R, Rule GS. 1995. A 3D ^{1}H, ^{15}N, and ^{13}C NOESY correlating experiment. J Magn Reson B 108:294–298.
40. Xia YL, Yee A, Arrowsmith CH, Gao XL. 2003. $^{1}H_{C}$ and $^{1}H_{N}$ total NOE correlations in a single 3D NMR experiment. ^{15}N and ^{13}C time-sharing in t_1 and t_2 dimensions for simultaneous data acquisition. J Biomol NMR 27:193–203.
41. Xu YQ, Long D, Yang DW. 2007. Rapid data collection for protein structure determination by NMR spectroscopy. J Am Chem Soc 129:7722–7723.
42. Wurtz P, Aitio O, Hellman M, Permi P. 2007. Simultaneous detection of amide and methyl correlations using a time shared NMR experiment: application to binding epitope mapping. J Biomol NMR 39:97–105.
43. Kupce E, Muhandiram DR, Kay L. 2003. A combined HNCA/HNCO experiment for ^{15}N labelled proteins with ^{13}C at natural abundance. J Biomol NMR 27:175–179.
44. Frueh DP, Arthanari H, Wagner G. 2005. Unambiguous assignment of NMR protein backbone signals with a time-shared triple-resonance experiment. J Biomol NMR 33:187–196.

BIOGRAPHIES

Teodor Parella was born in Sta. Coloma de Farners (Girona, Spain) in 1965. He obtained his B.Sc (1988) and Ph.D. (1993) at Universitat Autònoma de Barcelona (UAB). Now, he is the Manager of the NMR facility at UAB. He has published about 150 publications in international journals in the area of chemistry and NMR spectroscopy. Current research interest includes NMR pulse sequence development and applications of NMR to organic and organometallic compounds.

Pau Nolis was born in Badalona (Barcelona, Spain) in 1980. He obtained his B.Sc (2002), M.Sc (2004), and Ph.D. (2007) at Universitat Autònoma de Barcelona. His M.Sc was focused on assymetric Diels-Alder reaction under the supervision of professor Albert Virgili. Ph.D was focused on the development of NMR pulse sequences under the supervision of Dr. Teodor Parella. Currently working as research supporter NMR spectroscopist at the same university.